Minimum energy multiple crack propagation. Part I: Theory and state of the art review

Danas Sutula[a,b], Pierre Kerfriden[b], Tonie van Dam[a], and Stéphane P.A. Bordas[c,a,*]

[a]Institute of Computational Engineering, University of Luxembourg, 6 Avenue de la Fonte, 4362 Esch-sur-Alzette, Luxembourg
[b]School of Engineering, Cardiff University, Queen's Building, The Parade, Cardiff, CF24 3AA, UK
[c]Visiting Professor, Institute of Research and Development, Duy Tan University, K7/25 Quang Trung, Danang, Vietnam
[*]stephane.bordas@alum.northwestern.edu

July 17, 2017

Contents

Abstract

The three-part paper deals with energy-minimal multiple crack propagation in a linear elastic solid under quasi-static conditions. The principle of minimum total energy, i.e. the sum of the potential and fracture energies, which stems directly from the Griffith's theory of cracks, is applied to the problem of arbitrary crack growth in 2D. The proposed formulation enables minimisation of the total energy of the mechanical system with respect to the crack extension directions and crack extension lengths to solve for the evolution of the mechanical system over time. The three parts focus, in turn, on (I) the theory of multiple crack growth including competing cracks, (II) the discrete solution by the extended finite element method using the minimum-energy formulation, and (III) the aspects of computer implementation within the *Matlab* programming language. The key contributions of Part-I of this three-part paper are given as follows. (1) Formulation of the total energy functional governing multiple crack behaviour. (2) Three solution methods to the problem of competing crack growth for different fracture front stabilities, e.g. stable, unstable, or partially stable crack tip configurations; we compare our ap-

proach to [17] and demonstrate via example cases that the latter approach of resolving competing crack growth is not energy minimal in some cases. Finally, (3), the minimum energy criterion for a set of crack tip extensions is posed as the condition of vanishing rotational dissipation rates with respect to the extension angles. The proposed formulation lends itself to a straightforward application within a discrete framework involving multiple finite-length crack tip extensions. The open-source Matlab code, documentation, benchmark/example cases are included as supplementary material.

1 Introduction

Modelling fracture initiation and propagation is key to engineering design and has importance in a number of other fields, including biomechanics and surgical simulations [19]. The full complexity of the mechanical phenomena taking place during the fracture process is most commonly not taken into account and the vast majority of industrial fracture mechanics simulations consider a single crack under the assumptions of linear elastic fracture mechanics (LEFM) [10, 127, 128, 42, 44, 58]. Some notable problems of industrial significance that involve large numbers of interacting cracks include: silicon wafer splitting via the coalescence of multiple micro-cracks [28, 29, 37, 38], fatigue lifetime prediction of solder joints due to crack initiation and growth from thermal loading [109, 64, 63, 62], development of micro-crack toughened ceramics and composites [24, 25, 26, 5, 106], structural integrity assessment of reactor pressure vessels [21]. However, often-times in structural health monitoring the simpler (and more conservative) approach of analysing many closely spaced cracks is to replace the cracks by an equivalent (longer) crack [21] or apply simple superposition techniques, e.g. [47, 48, 49].

In spite of the clear importance of studying multi-crack problems, both crack initiation and crack interaction in dense cracking scenarios are much less studied than the single crack problem. The aim our three-part paper is to comprehensively deal with the case of arbitrary multi-crack growth in linear elastic solids. Specifically, Part-I of our three-part paper offers a detailed overview of the theoretical analysis of multi-crack growth problems and formulates the solution methods for solving arbitrary crack growth problems following the principle of energy minimality; then, Part-II present the description of the discrete solution methods; finally, Part-III describes our open-source computer implementation and also presents many benchmark problems for verifying our proposed solution strategies. The theory is directly applicable in the general three-dimensional case but our write-up is restricted to the two-dimensional setting.

The present paper, Part-I, provides insight into competing crack growth behaviour as well as several solution strategies for determining the relative growth rates of the competing crack tips. The problem to be solved is effectively a constrained quadratic programming problem with both equality and inequality constraints. We propose three solution methods, where each is applied based on the local behaviour of the total energy functional, which can be characterised in terms of the stability property of the fracture front

configuration. The second aim of this paper is to formulate the criterion for the crack growth direction based on the principle of minimum energy in a way that lends itself to application within a discrete framework. The key property of the criterion is that it does not depend on the crack tip field (e.g. the crack tip stress intensity factors). Thus, the present contribution mainly serves as a stepping stone for gaining insight into multiple crack propagation under minimum energy conditions and for, subsequently, formulating the discrete problem of multiple crack growth and solving it.

The text is organised as follows. Section-2 describes the model problem which is that of a 2D linear-elastic solid with multiple pre-existing cracks. Section-3 describes the representation of cracks. Section-4 reviews Griffith's crack growth law. Section-5 formulates the total energy functional that governs the behaviour of the mechanical system and explains how the minimisation of this functional leads to the equilibrium evolution of the mechanical system over time. Then, section-6 tackles the problem of competing crack growth. Section-7 formulates the crack growth direction criterion based on the principle of minimum total energy. Finally, a summary and conclusions are given.

2 Overview of computational fracture mechanics

2.1 Discrete versus continuum

All materials, if observed at a sufficiently small scale, can be considered discrete. Failure in solids can be modelled using such discrete approaches as: the discrete element method [75, 74, 76] or molecular dynamics [6, 129, 116, 16, 115, 114]. We focus here on continuum description of solids and refer to [115] for a review of recent approaches to continuum fracture mechanics and open-source software for continuum/molecular-dynamics coupling. The reader is referred to [117, 118] for quantum mechanical approaches.

2.2 Continuum approaches to fracture

Within the continuum context, there are two approaches to modelling failure processes. The problem is approached either from the viewpoint of *continuum damage mechanics* (CDM) [46, 98, 97, 77] or *fracture mechanics* (FM) [45, 122, 123, 2]. CDM considers a smeared crack model: weakening of the structure and failure are captured by strain localisation along the failure zone. FM, on the other hand, considers a discrete crack: a crack is modelled as a strong discontinuity in the displacement field. A zero-thickness discontinuity results in an infinitely sharp crack such that the state of stress exhibits a square-root singularity at the crack tip [45, 122, 123], which is difficult to deal with numerically. The accuracy of the tip fields is important because many classical crack growth criteria rely on these fields to determine how a crack evolves in space and time [131, 12, 99]. Different criteria may be concerned with different aspects of crack behaviour but a common denominator to all crack growth approaches is the requirement to determine

if a crack grows, by how much, and in which direction. In a three-dimensional setting, this problem has to be solved all along the entire crack front. More recent efforts have been focused on bridging this divide between continuum (damage) and discrete cracks through, for example, the variational theory of fracture [30, 13, 31, 20, 14, 30, 59, 65] or phase field models [110, 67, 66, 11, 1, 68].

2.3 Crack initiation and propagation

In linear elastic fracture mechanics (LEFM), the most well known criteria are: the maximum tangential stress (MTS) criterion [23, 15, 72, 71, 61] (also called the maximum hoop-stress criterion), the maximum energy release rate (MERR) criterion[85, 43, 125, 126, 124, 52, 40, 78], and the minimum strain energy density (MSED) criterion [108, 107]. The aforementioned criteria can be used to determine both the direction and the onset of crack growth. On the other hand, the criterion based on the principle of local symmetry (PLS) [34, 51, 41] can only be used to determine the direction of crack growth. A comparison of different criteria can be found in [103, 105, 12, 22, 99]. The reader may also wish to refer to the 2010 review on crack propagation algorithms [96, 93].

Note that LEFM is valid if the non-linear material behaviour (e.g. plastic deformation) is confined to a small region close to the crack tip. For materials that show considerable plasticity prior to crack growth, LEFM is no longer a suitable model and the elastic-plastic fracture mechanics (EPFM) approach should be used instead. Within the EPFM framework, there are two parameters that can be used to characterise the crack tip state: these are the J-integral [100] and the crack tip opening displacement (CTOD) [121]. Either one can be used as a fracture criterion as they show little size-dependence even for relatively large amounts of crack tip plasticity [119, 133]; furthermore, these criteria remain significant within the LEFM framework. Since the elastic-plastic material behaviour can be idealised as non-linearly elastic (assuming no unloading takes place), the J-integral value uniquely characterises the crack tip state. The critical J-integral value (J_{Ic}) is obtained at the point of failure of a specimen during an experiment.

Some materials can exhibit an increase in the fracture resistance with crack extension due to the expansion of the plastic region around the crack tip. A plot of the material's resistance to fracture versus crack length gives the material's fracture resistance curve (R-curve) [119, 133, 132]. For an ideally brittle material the R-curve is flat because the surface energy is a fixed material property; on the other hand, the fracture resistance of many tough materials tends to increase with crack length until a steady-state value is reached. Ideally, the initial J_{Ic} and the R-curve are properties of the material and do not depend on the size or shape of the cracked body. This is reasonably true when the plastic deformation at the crack tip is small relative to the specimen size.

2.4 Loss of material stability

Depending on the physics of the fracture problem, other criteria may be introduced to determine when a new crack should be nucleated or when an existing crack should bifurcate into multiple branches, e.g. using material stability analysis [82]. This has been applied to dynamic crack growth [130, 111, 11, 91, 94, 9, 92, 95]. However, with regard to crack nucleation, the classic linear-elastic theory of fracture mechanics predicts that an infinite stress is required to create a new crack inside an elastic solid [35, 36, 59]. Crack nucleation within FM has been attempted by applying non-local criteria such as maximum average stress [81, 104, 103] or maximum energy release [103, 54, 55]. For a comparison of different crack initiation criteria refer to [103, 105, 131] and to the 2010 review [93]. Alternatively, crack nucleation can be addressed within the CDM framework whereas FM can be applied to model sufficiently well developed smeared cracks as discrete cracks [3, 92, 8, 120].

2.5 Variational theories

A method of bridging the gap between continuum damage mechanics and fracture mechanics is provided by the *variational* approach to fracture, which is based on the fundamental principles of minimum energy [18, 30, 39, 102, 101, 27], irreversibility of the fracture path [57, 4, 39, 14], and energy conservation. The variational theory of brittle fracture was set out in [18, 30, 31] where the basic idea was to consider the fracture surface as an internal variable of the total energy functional whose variation induced an energy dissipation. Numerical implementations of the variational approach to fracture were presented in [13, 20, 14, 65] where a zero-width crack was replaced by a regularised (diffusive) fracture zone. The regularisation was in a form of a gradient of the internal variable. In principle, the fracture representation was similar to some early non-local gradient-enhanced continuum damage models [88, 32, 89, 56, 79]; however, in the present case, the regularised fracture zone converges to a discrete crack when the regularising parameter tends to zero [60, 33, 20].

More recently, two notable fracture modelling strategies have emerged following the variation principle and non-local continuum damage mechanics, namely: the phase-field model (PFM) [110, 67, 66, 11, 1, 68] and the thick level set (TLS) model [90, 70, 112, 8]. In PFM, the fracture zone is described by a global fracture surface functional whose minimum corresponds to an exponentially decaying damage function from where the crack is localised (i.e. location of full damage). As the regularisation length-scale tends to zero, the diffusive fracture surface converges to a sharp crack topology [60, 65]. The main advantage of PFM is that the evolution of the system is entirely governed by a single energy functional whose time-continuous minimisation in terms of the displacement field and the internal fracture surface variable yields the solution to the fracture evolution problem. In TLS, a level set function [84, 83] is used to separate the undamaged zone from the fully damaged zone by a characteristic width where the damage varies

monotonically, i.e. the damage variable is an explicit function of the level set. The propagation of the damage front is driven by the so-called *configurational force* [113, 39, 50] that corresponds to the vector of maximal energy dissipation with respect to the (regularised) extension of the front of the level set. The numerical representation of the fully damaged region can be enhanced by enriching the standard finite element approximation with a ramped Heaviside function to completely decouple the opposite sides of the fully damaged region [87, 7, 8]. Although the enrichment is not mandatory for TLS, it is beneficial especially for coarser meshes as the enrichment effectively removes any spurious cohesive tractions that may be transferred across the fully damaged zone by those nodes whose support bridges the fully damaged zone [70, 8, 69, 73, 86].

The main advantages of TLS are similar to those of PFM in that the method can naturally initiate cracks, propagate them, and handle crack merging and branching without relying on *ad hoc* criteria, such as in discrete crack representation. Thus, TLS and PFM are methods that effectively bridge the gap between continuum-damage mechanics and fracture mechanics. A comparison between the methods is given by [53].

2.6 Discussion

Some of the drawbacks of PFM and TLS models are similar to those of CDM based approaches; in particular, the methods share the high computational cost of the spatial discretisation that is needed to approximate a brittle crack via strain localisation since a crack is effectively modelled at the constitutive level via the degradation of material stiffness. This cost can be prohibitive if it is required to simulate complex crack patterns such as crack branching and merging with a high resolution. On the other hand, the main difficulty with the FM approach is that a crack needs to be defined within the continuum context at the level of the geometry, i.e. as a moving boundary of the solid, so that the problem governing PDE's make sense within the volume of the solid continuum. Hence, within the FM approach, it is necessary to manually track each crack and manage crack intersections as they occur. In addition, a crack growth criterion is required to determine when, where and which cracks propagate. Nonetheless, FM is a very competitive choice when it comes to modelling discrete cracks, despite the practical difficulties. The field of (linear-elastic) fracture mechanics is well-established and the state of the art numerical methods greatly facilitate the integration of arbitrary discontinuities within a continuum discretisation such that accurate fracture solutions are possible.

3 Model problem

Consider a two-dimensional (2D) brittle linear-elastic body $\Omega \subset \mathbb{R}^2$ in the (x, y)-plane, as depicted in Figure 1. The body has a boundary $\Gamma = \Gamma_u \cup \Gamma_t \cup \Gamma_c$, where Γ_u is the prescribed displacement (Dirichlet) boundary, Γ_t is the prescribed traction (Neumann) boundary on the exterior of the domain, and Γ_c is the prescribed traction (Neumann)

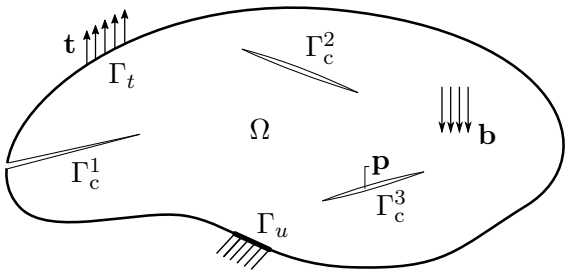

Figure 1: Diagram of a 2D model problem of a multiply cracked linear-elastic solid in static-equilibrium with the external loading action.

boundary on the fracture surfaces; note that $\Gamma_u \neq \emptyset$ and that the boundaries are subdivided such that $\Gamma_u \cap \Gamma_t \cap \Gamma_c = \emptyset$. Γ_c is assumed to constitute n_{crk} fracture surfaces such that $\Gamma_c = \Gamma_{c1} \cup \Gamma_{c2} \cup \cdots \cup \Gamma_{cn_c}$. The 2D static-equilibrium equations (1) and boundary conditions (2)-(3) can be summarised as follows (note, $i, j = 1, 2$):

$$\sigma_{ij,j} = b_i \quad \text{in } \Omega \tag{1}$$
$$u_i = \bar{u}_i \quad \text{on } \Gamma_u \tag{2}$$
$$\sigma_{ij}\, n_j = t_i \quad \text{on } \Gamma_t \tag{3}$$
$$\sigma_{ij}\, n_j = p \quad \text{on } \Gamma_c \tag{4}$$

where σ_{ij} is the Cauchy stress tensor component; b_i – body force; u_i – displacement; n_i – unit (outward) normal to boundary Γ; $\bar{u}_i$ – prescribed displacement on Γ_u; t_i – prescribed traction on Γ_t; p – prescribed pressure normal to fracture surface Γ_c. The stress-strain relationship for a linear-elastic solid can be given by Hooke's law:

$$\sigma_{ij} = C_{ijkl}\, \varepsilon_{kl} \quad i, j, k, l \in \{1, 2\} \tag{5}$$

where C_{ijkl} is the component of the symmetric 4^{th}-order constitutive tensor for an isotropic material, and ε_{kl} is the component of the small-deformation strain tensor:

$$\varepsilon_{ij} = \frac{1}{2}(u_{i,j} + u_{j,i}) \quad i, j \in \{1, 2\} \tag{6}$$

The constitutive tensor $\mathbf{C}$ can also be given in matrix form, according to the type of a 2D problem at hand:

$$\mathbf{C} \equiv \begin{bmatrix} C_{xxxx} & C_{xxyy} & C_{xxxy} \\ C_{yyxx} & C_{yyyy} & C_{yyxy} \\ C_{xyxx} & C_{xyyy} & C_{xyxy} \end{bmatrix} = \begin{cases} \frac{E}{1-\nu^2} \begin{bmatrix} 1 & \nu & 0 \\ \nu & 1 & 0 \\ 0 & 0 & \frac{1-\nu}{2} \end{bmatrix} & \text{Plane-stress} \\ \frac{E}{(1+\nu)(1-2\nu)} \begin{bmatrix} 1-\nu & v & 0 \\ \nu & 1-\nu & 0 \\ 0 & 0 & \frac{1-2\nu}{2} \end{bmatrix} & \text{Plane-strain} \end{cases} \tag{7}$$

where the two material constants E and ν are, respectively, the Young's modulus of elasticity and the Poisson's ratio.

The principle of virtual work that governs the elasto-static equilibrium problem can be stated as follows. Find $\mathbf{u} \in \mathcal{U}$ such that for any virtual displacement $\delta\mathbf{u} \in \mathcal{U}_0$ the equality between the internal and the external virtual works is satisfied, i.e.

$$\forall \delta\mathbf{u} \in \mathcal{U}_0 \quad \int_\Omega \varepsilon_{ij}(\delta\mathbf{u}) C_{ijkl} \varepsilon_{kl}(\mathbf{u}) \, \mathrm{d}V = \int_{\Gamma_t} \delta u_i t_i \, \mathrm{d}A + \int_{\Gamma_c} \delta[\![u_i]\!] n_i p \, \mathrm{d}A \tag{8}$$

The admissible trial space of displacements $\mathcal{U}$ and the test space of the virtual displacements $\mathcal{U}_0$ are defined respectively as:

$$\mathcal{U} = \{ \ \mathbf{u} \in H^1(\Omega \backslash \Gamma_\mathrm{c}) : \ \mathbf{u}|_{\Gamma_u} = \bar{\mathbf{u}} \text{ and } [\![u_i]\!] \cdot n_i \geq 0 \text{ on } \Gamma_\mathrm{c} \} \tag{9}$$

$$\mathcal{U}_0 = \{ \delta\mathbf{u} \in H^1(\Omega \backslash \Gamma_\mathrm{c}) : \delta\mathbf{u}|_{\Gamma_u} = \mathbf{0} \text{ and } [\![\delta u_i]\!] \cdot n_i \geq 0 \text{ on } \Gamma_\mathrm{c} \} \tag{10}$$

where H^1 is the Sobolev space of real vector-valued continuous functions with first square-integrable generalised derivatives on the part of the domain given by $\Omega \backslash \Gamma_\mathrm{c}$. Note that the admissible trial and test spaces are assumed to respect the constraint of no crack surface interpenetration. As our implementation does not explicitly enforce this constraint (e.g. by means of resolving the contact mechanics problem in the event contact is detected) we focus on fracture problems driven by tensile loading.

4 Representation of cracks

In describing the evolution of multiple cracks it is practical to consider unique crack branches that stem from the tips of each pre-existing crack. This, in turn, simplifies the association of a particular crack tip branch $i \in \{1, 2, \ldots, n_\mathrm{tip}\}$ with its energy release rate $G_{\mathrm{s}i}$. We will denote the set of pre-existing cracks by $\mathcal{I}_\mathrm{c} = \{1, 2, \ldots, n_\mathrm{c}\}$ and the set of crack tip branches by $\mathcal{I}_\mathrm{tip} = \{1, 2, \ldots, n_\mathrm{tip}\}$. It is assumed that the number of crack tips can be related to the number of cracks via $n_\mathrm{tip} = 2n_\mathrm{c}$ and that the beginning and end of a particular crack $i \in \mathcal{I}_\mathrm{c}$ corresponds to the crack tips $2i - 1$ and $2i$ respectively. In this reference frame (see Figure 2), a crack $i \in \mathcal{I}_\mathrm{c}$ is considered to have a pre-existing

fracture area a_{0i}, whereas a crack tip branch $i \in \mathcal{I}_{\text{tip}}$ is supposed to have a time-dependent fracture area ℓ_i. Thus, prior to the start of the fracture process, the fracture area of any branch is supposed to be zero, i.e. $\ell_i = 0 \, \forall i \in \mathcal{I}_{\text{tip}}$, whereas upon the start of the fracture process, the branch areas can be greater than zero, i.e. $\ell_i \geq 0 \, \forall i \in \mathcal{I}_{\text{tip}}$.

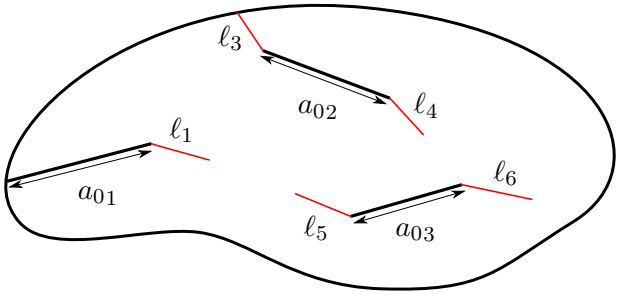

Figure 2: The proposed crack representation scheme. A pre-existing crack is assumed to have a fixed length a_{0i} where $i \in \mathcal{I}_{\text{c}}$. The length of a crack tip branch, which is assumed to evolve over time, is ℓ_j where $j \in \mathcal{I}_{\text{tip}}$.

Within this crack representation, the total area a_i of a crack $i \in \mathcal{I}_{\text{c}}$ is determined as the sum of its initial area a_{0i} and the areas of the two of its branches, ℓ_{2i-1} and ℓ_{2i}:

$$i \in \mathcal{I}_{\text{c}} \quad a_i = a_{0i} + \ell_{2i-1} + \ell_{2i} \tag{11}$$

Similarly, the total cracked area is computed as:

$$a = \sum_{i=1}^{n_{\text{c}}} a_i = \sum_{i=1}^{n_{\text{c}}} a_{0i} + \sum_{i=1}^{n_{\text{tip}}} \ell_i \tag{12}$$

The growth rate $\hat{\ell}_i$ of a crack branch $i \in \mathcal{I}_{\text{tip}}$ is defined as the increase in the area of the branch ($\delta \ell_i$) relative to the increase in the total cracked area ($\delta a = \sum_{i \in \mathcal{I}_{\text{tip}}} \delta \ell_i$):

$$\forall i \in \mathcal{I}_{\text{tip}} \quad \hat{\ell}_i = \frac{\mathrm{d}\ell_i}{\mathrm{d}a} \geq 0 \tag{13}$$

Note that crack growth irreversibility is implied by the inequality sign. Consequently, the space of admissible branch growth rates $\mathcal{A}$ (i.e. $\hat{\boldsymbol{\ell}} \in \mathcal{A}$) can be defined as:

$$\mathcal{A} = \left\{ \hat{\boldsymbol{\ell}} : \forall i \in \mathcal{I}_{\text{tip}}, \ \hat{\ell}_i \in [0, 1] \text{ subject to } \textstyle\sum_{i \in \mathcal{I}_{\text{tip}}} \hat{\ell}_i = 1 \right\} \tag{14}$$

5 Griffith's crack growth law

According to Griffith [35, 36], the energy release rate $G_{\mathrm{s}i}$ of a crack tip $i \in \mathcal{I}_{\mathrm{tip}}$ is defined as the rate of strain energy release $(-\mathrm{d}U_{\mathrm{s}}/\mathrm{d}\ell_i)$ plus the rate of external work done $(\mathrm{d}W_{\mathrm{ext}}/\mathrm{d}\ell_i)$ with respect to the extension of the crack tip branch area ℓ_i:

$$G_{\mathrm{s}i} = -\frac{\mathrm{d}U_s}{\mathrm{d}\ell_i} + \frac{\mathrm{d}W_{\mathrm{ext}}}{\mathrm{d}\ell_i} \tag{15}$$

Since the potential energy Π of an elastic solid is equal to the sum of the internal strain energy U_{s} and the external load potential $(-V)$, and given that for a constant external load a decrease in the load potential is equal to an increase in the external work W_{ext}, the crack tip energy release rate must equal the rate of potential energy decrease:

$$G_{\mathrm{s}i} = -\frac{\mathrm{d}U_{\mathrm{s}}}{\mathrm{d}\ell_i} - \frac{\mathrm{d}V}{\mathrm{d}\ell_i} \tag{16}$$

$$G_{\mathrm{s}i} = -\frac{\mathrm{d}\Pi}{\mathrm{d}\ell_i}, \tag{17}$$

In the general case of multi-crack growth, the mean energy release rate G_{s} with respect to a set of given crack tip extension rates $\hat{\boldsymbol{\ell}} \in \mathcal{A}$ can be computed as follows:

$$G_{\mathrm{s}} = -\frac{\mathrm{d}\Pi}{\mathrm{d}a} \tag{18}$$

$$G_{\mathrm{s}} = G_{\mathrm{s}i}\frac{\mathrm{d}\ell_i}{\mathrm{d}a} \tag{19}$$

$$G_{\mathrm{s}} = G_{\mathrm{s}i}\hat{\ell}_i \tag{20}$$

If the fracture toughness of a material happens to vary spatially such that $G_{\mathrm{c}i} \neq G_{\mathrm{c}j}$ if $i \neq j$ for $i, j \in \mathcal{I}_{\mathrm{tip}}$, the equivalent G_{c} (i.e. the equivalent resistance of the material with respect to a particular fracture growth $\hat{\boldsymbol{\ell}} \in \mathcal{A}$) is determined analogously to (20):

$$G_{\mathrm{c}} = G_{\mathrm{c}i}\hat{\ell}_i \tag{21}$$

The onset of crack growth occurs at the instance the fracture driving force G_{s} overcomes the material resistance G_{c}. Thus, the Griffith's crack growth criterion is stated as:

$$\forall \hat{\boldsymbol{\ell}} \in \mathcal{A} \quad \begin{cases} (G_{\mathrm{s}i} - G_{\mathrm{c}i})\,\hat{\ell}_i < 0 & \text{(no growth)} \\ (G_{\mathrm{s}i} - G_{\mathrm{c}i})\,\hat{\ell}_i = 0 & \text{(growth)} \end{cases} \tag{22}$$

where the driving energy release rate $G_{\mathrm{s}} = G_{\mathrm{s}i}\hat{\ell}_i$ is implicitly bounded (from above) by the critical energy release rate $G_{\mathrm{c}} = G_{\mathrm{c}i}\hat{\ell}_i$ to ensure the material state makes physical sense, i.e. the material's ability to resist fracture growth is not exceeded by the fracture driving force. In other words, the physical constraint that is implied in (22) is:

$$\forall i \in \mathcal{I}_{\mathrm{tip}} \quad G_{\mathrm{s}i} \leq G_{\mathrm{c}i} \tag{23}$$

If a given crack growth $\hat{\boldsymbol{\ell}}_{\mathrm{c}} \in \mathcal{A}$ satisfies the growth condition in (22) then $\hat{\boldsymbol{\ell}}_{\mathrm{c}}$ is a critical solution that satisfies the following inequality condition with respect to any $\hat{\boldsymbol{\ell}} \in \mathcal{A}$:

$$\left(G_{\mathrm{s}i} - G_{\mathrm{c}i}\right)\hat{\ell}_{\mathrm{c}i} \geq \left(G_{\mathrm{s}i} - G_{\mathrm{c}i}\right)\hat{\ell}_i \tag{24}$$

It is implied by (24) that at the instance of crack growth the dissipation-like term:

$$\mathcal{D}(\hat{\boldsymbol{\ell}}) \equiv \left(G_{\mathrm{s}i} - G_{\mathrm{c}i}\right)\hat{\ell}_i \tag{25}$$

will be maximum (and, under energy conservation conditions, equal to zero). Conversely, the critical crack growth solution will satisfy:

$$\hat{\boldsymbol{\ell}}_{\mathrm{c}} = \underset{\hat{\boldsymbol{\ell}} \in \mathcal{A}}{\arg\max}\, \mathcal{D}(\hat{\boldsymbol{\ell}}), \tag{26}$$

By extension, the critical fracture path: $\boldsymbol{\ell}_{\mathrm{c}} = \int_{a_0}^{a_\infty} \hat{\boldsymbol{\ell}}\, \mathrm{d}a$ will be one that maximises $\mathcal{D}(\hat{\boldsymbol{\ell}})$ with respect to $\hat{\boldsymbol{\ell}} \in \mathcal{A}$ at every instance of the evolution of the total fractured area $a \in [a_0, a_\infty]$, where a_0 and a_∞ are the initial and the final fractured areas.

6 The total energy function

Following from the fact that the critical fracture path produces maximal dissipation, it is possible to write down a total energy function $\mathcal{E} = \mathcal{E}(\boldsymbol{\ell})$ whose time-continuous minimisation, in terms of the cracked area $\boldsymbol{\ell}$, would give the solution to the critical fracture path. The first step to obtaining $\mathcal{E}$ is to define the following relationship:

$$-\frac{\mathrm{d}\mathcal{E}}{\mathrm{d}a} = \mathcal{D}(\hat{\boldsymbol{\ell}}), \tag{27}$$

which states that the decrease rate of $\mathcal{E}$ with respect to an increasing total cracked area a is equal to the surplus energy per unit cracked area that is available for dissipation. $\mathcal{E}(\boldsymbol{\ell})$ can then be obtained by integrating equation (27) with respect to a:

$$\mathcal{E}(\boldsymbol{\ell}) = \int (-G_{\mathrm{s}i} + G_{\mathrm{c}i})\, \hat{\ell}_i \, \mathrm{d}a \tag{28}$$

$$\mathcal{E}(\boldsymbol{\ell}) = \int \left(\frac{\mathrm{d}\Pi}{\mathrm{d}\ell_i} + G_{\mathrm{c}i} \right) \mathrm{d}\ell_i \tag{29}$$

$$\mathcal{E}(\boldsymbol{\ell}) = \Pi(\mathbf{u}(\boldsymbol{\ell}), \boldsymbol{\ell}) + \int G_{\mathrm{c}i}(\boldsymbol{\ell}) \, \mathrm{d}\ell_i \tag{30}$$

where the displacement field $\mathbf{u}$ is considered as a function of $\boldsymbol{\ell}$. Fracture growth can occur if $\mathcal{E}(\boldsymbol{\ell})$ can decrease or stay constant with increasing $\boldsymbol{\ell}$. The critical fracture path is obtained by minimising $\mathcal{E}(\boldsymbol{\ell})$ with respect to $\boldsymbol{\ell}$ such that $\mathcal{E}(\boldsymbol{\ell})$ follows the path of steepest descent with respect to $\boldsymbol{\ell}$. Note that the present form of the total energy functional does not distinguish between compressive and tensile cracks in so far as achieving total energy minimality of the evolution of the mechanical system is concerned, i.e. the growth of both types of crack is energetically equivalent. However, we make the assumption that the growth of compressive cracks is unfavourable (for various reasons, e.g. the material may be much tougher in compression). The reason behind this assumption is the limitation of our model to account for cracks in compression as we do not explicitly enforce the constraint of no crack surface interpenetration. Even though the energy functional (30) can easily take into account crack surface loading (such as due to internal crack pressure), the solution to the contact problem is beyond the aim of the present work. Thus, we focus on fracture problems driven by tensile loading. In cases of multiple cracks, the assumption of no crack surface interpenetration may be difficult to satisfy and, thus, some crack surface interpenetration will inevitably occur. Our way of handling cracks in compression is to simply deactivate them, i.e. if the (opening) mode-I stress intensity factor is negative, the crack tip is frozen for the particular step in time.

6.1 Total energy minimisation

The evolution of cracks is determined by the time-continuous minimisation of the total energy function $\mathcal{E}(\boldsymbol{\ell})$. So far, the problem of fracture growth has been considered without invoking the equilibrium state of the solid. Now we consider the problem of crack evolution such that it is consistent with the equations of static-equilibrium (8).

In the definition of $\mathcal{E}(\boldsymbol{\ell})$ in equation (30), the potential energy was written as $\Pi(\mathbf{u}(\boldsymbol{\ell}), \boldsymbol{\ell})$. The relationship between $\mathbf{u}$ and $\boldsymbol{\ell}$ is imposed by the equations of static-equilibrium; specifically, $\Pi(\mathbf{u}, \boldsymbol{\ell})$ is required to be minimised (stationary) with respect to $\mathbf{u}$ for a given fracture boundary Γ_{c}, which can be parametrised in terms of $\boldsymbol{\ell}$. The relationship

$\mathbf{u} = \mathbf{u}(\boldsymbol{\ell})$ is embedded in the solution to the variational form (8) of static-equilibrium, which can be stated in terms of a stationary potential energy:

$$\left.\frac{\partial \Pi}{\partial \mathbf{u}}\right|_{\Gamma_{\mathrm{c}}(\boldsymbol{\ell})} = \mathbf{0} \tag{31}$$

Although a closed-form relationship between $\mathbf{u}$ and $\boldsymbol{\ell}$ is not generally available, it is possible to explicitly resolve the differential relationship $\mathrm{d}\mathbf{u}/\mathrm{d}\boldsymbol{\ell}$. To this end, it is only necessary to suppose that the condition of static-equilibrium is satisfied during an infinitesimal crack extension $\delta\boldsymbol{\ell} = \hat{\boldsymbol{\ell}}\,\delta a$. Consequently, we have:

$$\begin{aligned} \forall i \in \mathcal{I}_{\mathrm{tip}} \quad & \frac{\mathrm{d}}{\mathrm{d}\ell_i}\left(\frac{\partial \Pi}{\partial \mathbf{u}}\right) = \mathbf{0} \\ & \frac{\partial}{\partial \ell_i}\left(\frac{\partial \Pi}{\partial \mathbf{u}}\right) + \frac{\partial^2 \Pi}{\partial \mathbf{u}^2}\frac{\mathrm{d}\mathbf{u}}{\mathrm{d}\ell_i}^{\mathrm{T}} = \mathbf{0} \\ & \frac{\mathrm{d}\mathbf{u}}{\mathrm{d}\ell_i} = -\frac{\partial}{\partial \ell_i}\left(\frac{\partial \Pi}{\partial \mathbf{u}}\right)^{\mathrm{T}}\left(\frac{\partial^2 \Pi}{\partial \mathbf{u}^2}\right)^{-1} \end{aligned} \tag{32}$$

where $\mathbf{u} = [u_x, u_y]$, $\frac{\partial}{\partial \mathbf{u}} = \left[\frac{\partial}{\partial u_x}, \frac{\partial}{\partial u_y}\right]^{\mathrm{T}}$ and $\frac{\partial^2}{\partial \mathbf{u}^2} = \frac{\partial}{\partial \mathbf{u}}\frac{\partial}{\partial \mathbf{u}}^{\mathrm{T}}$. In assuming that the solid is in a state of static-equilibrium, the computation of the rate of change of the total energy function $\left(-\frac{\mathrm{d}\mathcal{E}}{\mathrm{d}a}\big|_{\hat{\boldsymbol{\ell}}}\right)$ can be made simpler; this specifically affects to the determination of the fracture driving force G_{s}. Continuing from equation (17), the fundamental relationship between $G_{\mathrm{s}i}$ and the rate of change of $\Pi(\mathbf{u}(\boldsymbol{\ell}), \boldsymbol{\ell})$ in terms of the area ℓ_i of a specific crack tip branch $i \in \mathcal{I}_{\mathrm{tip}}$, can be revised as follows:

$$\begin{aligned} G_{\mathrm{s}i} &= -\frac{\mathrm{d}\Pi}{\mathrm{d}\ell_i} \\ G_{\mathrm{s}i} &= -\frac{\partial \Pi}{\partial \ell_i} - \frac{\mathrm{d}\mathbf{u}}{\mathrm{d}\ell_i}\frac{\partial \Pi}{\partial \mathbf{u}} \\ G_{\mathrm{s}i} &= -\frac{\partial \Pi}{\partial \ell_i} \end{aligned} \tag{33}$$

The result of (33) is that the total derivative that appeared in equation (17) for $G_{\mathrm{s}i}$ is now reduced to a partial derivative. Accordingly, G_{s} is determined based solely on the geometrical variations of the fracture surface $\Gamma_{\mathrm{c}}(\boldsymbol{\ell})$ and the material domain $\Omega(\boldsymbol{\ell})$, as affected by $\delta\boldsymbol{\ell}$. Combining the principles of maximal dissipation of the fracture path (26) and minimum potential energy the solid (8) enables the complete description the evolution of the mechanical system in terms of $\mathbf{u}$ and $\boldsymbol{\ell}$. This is achieved by minimising total energy function $\mathcal{E}(\mathbf{u}, \boldsymbol{\ell})$ with respect to $\mathbf{u}$ and $\boldsymbol{\ell}$ over the course of the evolution of the total fractured area $a \in [a_0, a_\infty]$. At any time in the fracture evolution process:

1. the total energy of the solid $\mathcal{E}(\mathbf{u}, \boldsymbol{\ell})$ needs to be minimised with respect to the displacement field $\mathbf{u}$ for static-equilibrium to hold true, and
2. in the state of static-equilibrium, the evolution of the cracked areas $\boldsymbol{\ell}$ is such that the total energy $\mathcal{E}(\mathbf{u}, \boldsymbol{\ell})$ follows the path of steepest descent,

Thus, the evolution of the mechanical system is determined by the time-continuous minimisation of $\mathcal{E}(\mathbf{u}, \boldsymbol{\ell})$ in terms of the variable pair $\{\mathbf{u}, \boldsymbol{\ell}\}$. Based on this formulation, the fractures and the equilibrium material state can evolve naturally insofar as $\mathcal{E}(\mathbf{u}, \boldsymbol{\ell})$ can be minimised in terms of $\{\mathbf{u}, \boldsymbol{\ell}\}$ for the given external load application.

6.2 Energy conservation

The crack growth formulation based on the total energy minimisation considers fixed boundary conditions at every point in time in the evolution process. At a given instance, crack growth is favourable provided that the total energy function can decrease or stay constant. The former condition is not energy conserving because it implies that there is more energy being liberated than is converted to fracture surface energy. On the contrary, crack growth that is characterised by a constant total energy function upholds the energy conservation principle such that the rate of energy liberation exactly matches the rate of energy dissipation via fracture surface creation. Although energy conservation does not affect the fracture path *per se*, in order to respect the energy conservation principle, the external load is required to adapt appropriately such that the total energy stays constant during the evolution of the mechanical system. Under these conditions, fracture growth can be considered as *just possible*. For simplicity, it will be supposed that the external load $\mathbf{t}$ is obtained by scaling a reference load $\mathbf{t}_0$ by a factor λ_t, i.e. $\mathbf{t} = \lambda_t \mathbf{t}_0$. For a linear-elastic solid, its potential energy is proportional to the square of the magnitude of the applied load. The same holds for the crack tip energy release rates. Assuming $G_{\mathrm{s}i} = G_{\mathrm{s}i}(\mathbf{t}_0)$, the load-factor λ_t for a particular crack growth configuration $\hat{\boldsymbol{\ell}} \in \mathcal{A}$ under energy conservation conditions is obtained as:

$$\lambda_t = \sqrt{\frac{G_{\mathrm{c}i}\hat{\ell}_i}{G_{\mathrm{s}i}\hat{\ell}_i}}, \quad \text{where } i \in \mathcal{I}_{\mathrm{tip}} \tag{34}$$

7 Competing crack growth

Concerning the problem of multi-crack growth, it is possible that under certain geometrical and loading conditions the maximum dissipation rate $\mathcal{D}_i = G_{\mathrm{s}i} - G_{\mathrm{c}i}$ is attained at several crack tips $\mathcal{I}^{\mathrm{c}}_{\mathrm{tip}} \subseteq \mathcal{I}_{\mathrm{tip}}$ simultaneously, i.e. $\mathcal{D}_i = \mathcal{D}_j \; \forall i, j \in \mathcal{I}^{\mathrm{c}}_{\mathrm{tip}}$. For this so-called problem of *competing crack growth* (CCG), a unique crack growth solution based on the maximum dissipation rate can not be determined because any admissible combination

of the critical crack tip extension rates gives an equivalent energy dissipation rate, i.e. $\mathcal{D}(\hat{\boldsymbol{\ell}}) = \text{const.}\ \forall \hat{\boldsymbol{\ell}} \in \mathcal{A}_\text{c}$, where $\mathcal{A}_\text{c} = \mathcal{A}(\mathcal{I}^\text{c}_\text{tip})$ is the space of admissible crack tip extension rates regarding the set of critical crack tips $\mathcal{I}^\text{c}_\text{tip} \subseteq \mathcal{I}_\text{tip}$. For this reason, it is necessary to consider the rate at which the dissipation rate changes with respect to the growth rates of the critical crack tips. Say, if $\hat{\boldsymbol{\ell}} = \{\hat{\ell}_i\}$, where $i \in \mathcal{I}^\text{c}_\text{tip}$, is a set of critical crack tip growth rates, then the rate of change of the energy dissipation is computed as follows:

$$\left.\frac{\mathrm{d}\mathcal{D}}{\mathrm{d}a}\right|_{\hat{\boldsymbol{\ell}}} = -\frac{\partial^2 \mathcal{E}(\boldsymbol{\ell})}{\partial \ell_i \partial \ell_j} \hat{\ell}_i \hat{\ell}_j \tag{35}$$

$$\left.\frac{\mathrm{d}\mathcal{D}}{\mathrm{d}a}\right|_{\hat{\boldsymbol{\ell}}} = \left(-\frac{\partial^2 \Pi(\boldsymbol{\ell})}{\partial \ell_i \partial \ell_j} + \frac{\mathrm{d}G_{\mathrm{c}i}}{\mathrm{d}\ell_j}\right) \hat{\ell}_i \hat{\ell}_j \tag{36}$$

The solution to the CCG problem in terms of the critical crack tip growth rates $\hat{\boldsymbol{\ell}}_\text{c} \in \mathcal{A}_\text{c}$, is determined as the one that maximises the rate at which the dissipation rate changes:

$$\hat{\boldsymbol{\ell}}_\text{c} = \underset{\hat{\boldsymbol{\ell}} \in \mathcal{A}_\text{c}}{\arg\max} \left.\frac{\mathrm{d}\mathcal{D}}{\mathrm{d}a}\right|_{\hat{\boldsymbol{\ell}}} \tag{37}$$

Before the solution methods to the CCG problem are described, it is useful to address the concept of *fracture stability*, which is characterised by the sign of $\frac{\mathrm{d}\mathcal{D}}{\mathrm{d}a}$, as it plays an important part in the solution approach to be used to solve a CCG problem.

7.1 Stability of cracks

The term $\mathrm{d}\mathcal{D}/\mathrm{d}a$ defined in (36) describes the property of stability of a fracture extension. The concept of fracture growth stability refers two possible fracture growth regimes, namely: one that is *stable* and one that is *unstable*. The terms are respectively used to describe a decreasing and an increasing (or an otherwise constant) dissipation rate:

$$\text{stable growth}: \quad \left.\frac{\mathrm{d}\mathcal{D}}{\mathrm{d}a}\right|_{\hat{\boldsymbol{\ell}}} < 0 \tag{38}$$

$$\text{unstable growth}: \quad \left.\frac{\mathrm{d}\mathcal{D}}{\mathrm{d}a}\right|_{\hat{\boldsymbol{\ell}}} \geq 0 \tag{39}$$

The significance of fracture stability, for a crack tip near the threshold of satisfying the fracture growth criterion is as follows. If fracture growth is stable (38) then given a small load increment there exists an equilibrium fracture front position that the crack tip will advance to and subsequently arrest. Conversely, if fracture growth is unstable

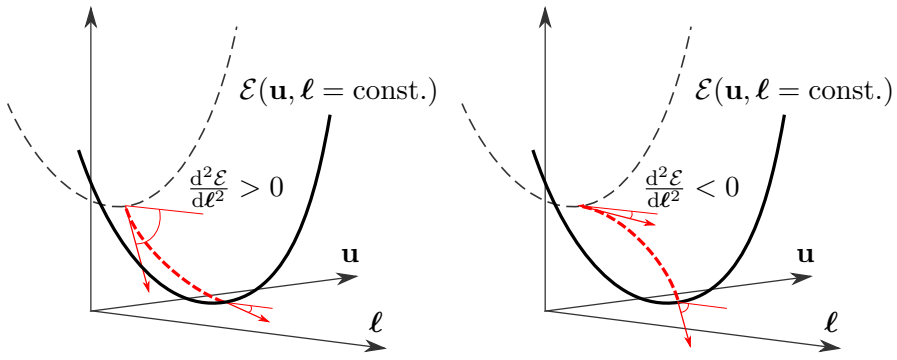

(a) Stable crack growth: $\frac{\mathrm{d}\mathcal{D}}{\mathrm{d}\boldsymbol{\ell}} < 0$ (b) Unstable crack growth: $\frac{\mathrm{d}\mathcal{D}}{\mathrm{d}\boldsymbol{\ell}} > 0$

Figure 3: Stable (a) and unstable (b) crack growth regimes showing the corresponding behaviours of the energy function $\mathcal{E}(\mathbf{u}(\boldsymbol{\ell}), \boldsymbol{\ell})$. Note that a decreasing total energy function simply means that there is available energy for crack growth, given the assumed load.

(39), an equilibrium fracture front position does not exist upon the application of a load increment. Thus, in the unstable case (39), crack growth may persist indefinitely. Nonetheless, for some tough materials the fracture driving force may well be increasing with crack length, however, crack growth can still be stable provided the material's resistance to crack growth increases at a faster rate than the driving force.

The classification of fracture growth stability can also serve as a means to interpret the local curvature of the total energy function $\mathcal{E}(\boldsymbol{\ell}) = \mathcal{E}\big(\mathbf{u}(\boldsymbol{\ell}), \boldsymbol{\ell}\big)$ with respect to $\boldsymbol{\ell}$. Figure 3 illustrates two different behaviours of $\mathcal{E}(\boldsymbol{\ell})$ corresponding to a stable and an unstable evolutions of cracks. However, in order to characterise the shape of $\mathcal{E}(\boldsymbol{\ell})$ with respect to all tip perturbations that preserve the current fracture area, the following three cases can be defined in reference to the stability property of the fracture *front*:

$$\text{unstable fracture front}: \quad \frac{\partial^2\mathcal{E}}{\partial\ell_i\partial\ell_j}\delta\ell_i\delta\ell_j \leq 0, \quad \forall\delta\boldsymbol{\ell} \in \mathbb{R}^n \text{ s.t. } \textstyle\sum_{i=1}^n \delta\ell_i = 0 \tag{40}$$

$$\text{stable fracture front}: \quad \frac{\partial^2\mathcal{E}}{\partial\ell_i\partial\ell_j}\delta\ell_i\delta\ell_j > 0, \quad \forall\delta\boldsymbol{\ell} \in \mathbb{R}^n \text{ s.t. } \textstyle\sum_{i=1}^n \delta\ell_i = 0 \tag{41}$$

$$\text{partially stable front}: \quad \frac{\partial^2\mathcal{E}}{\partial\ell_i\partial\ell_j}\delta\ell_i\delta\ell_j \geq 0, \quad \exists\delta\boldsymbol{\ell} \in \mathbb{R}^n \text{ s.t. } \textstyle\sum_{i=1}^n \delta\ell_i = 0 \tag{42}$$

Thus, a stable fracture front corresponds to a convex $\mathcal{E}(\boldsymbol{\ell})$, an unstable front is associated with a concave $\mathcal{E}(\boldsymbol{\ell})$, whereas a partially stable front results when $\mathcal{E}(\boldsymbol{\ell})$ is a generalised saddle function. As indicated in (40)-(42), the fractured area is supposed to stay constant with respect to any fracture front perturbation $\delta\boldsymbol{\ell}$, i.e. $\sum \delta\boldsymbol{\ell} = 0$. As such, the admissible crack tip perturbations include both positive and negative variations in the crack branch areas such that upon summing them all, the net change in fractured area is zero.

The behaviour of $\mathcal{E}(\boldsymbol{\ell})$ is important to the solution approach to be used to solve the CCG problem. Because a unique solution to the crack tip growth rates is not possible based on the maximum dissipation rate alone, it becomes necessary to consider the rate at which the dissipation rate changes. This leads to a constrained quadratic optimisation problem for which a closed-form analytical solution is generally difficult. An efficient numerical technique will typically exploit the properties of the curvature of $\mathcal{E}(\boldsymbol{\ell})$, i.e. the stability property of the critical part of the fracture front (40)-(42). The following section describes three viable strategies for solving the CCG problem.

7.2 Crack growth solution

The solution to the competing crack growth (CCG) problem are the crack tip extension rates $\hat{\boldsymbol{\ell}} \in \mathcal{A}_{\mathrm{c}}$ that maximise the rate at which the dissipation rate changes (37). From a mathematical viewpoint, the CCG problem can be considered as a constrained quadratic optimisation problem since the crack tip extension rates appear in a quadratic form in the expression of $\frac{\mathrm{d}\mathcal{D}}{\mathrm{d}a}$ in equation (36), and the constraints on the solution arise from having to consider the admissible space of the critical crack tip extension rates $\mathcal{A}_{\mathrm{c}}$. Specifically, the constraints are as follows: (1) the crack tip growth rates must add-up to one (i.e. $\sum_{i \in \mathcal{I}^{\mathrm{c}}_{\mathrm{tip}}} \hat{\ell}_i = 1$), and (2) the growth rates must be non-negative (i.e. $\hat{\ell}_i \geq 0 \ \forall i \in \mathcal{I}^{\mathrm{c}}_{\mathrm{tip}}$). Thus, the CCG problem can be stated as follows:

$$\begin{aligned} \text{objective}: \quad & \max \Psi(\boldsymbol{v}) = \frac{1}{2} H_{\mathrm{s}ij} v_i v_j \\ \text{subject to}: \quad & C(\boldsymbol{v}) \equiv v_i \mathbf{e}_i - 1 = 0, \\ & v_i \geq 0 \quad \forall i \in \mathcal{I}^{\mathrm{c}}_{\mathrm{tip}} \end{aligned} \tag{43}$$

In (43), the objective function to be maximised is $\Psi(\boldsymbol{v})$. The constraint of a unit fracture growth rate that any valid solution $\boldsymbol{v}$ needs to satisfy is enforced via the equality constraint equation $C(\boldsymbol{v}) = 0$. In addition, the constraint of a non-negative fracture growth rate is imposed via the inequality constraint $v_i \geq 0$, where $i \in \mathcal{I}^{\mathrm{c}}_{\mathrm{tip}}$. The factor "1/2" is introduced purely for the sake of convenience. Finally, the constant terms $H_{\mathrm{s}ij}$, where $i, j \in \mathcal{I}^{\mathrm{c}}_{\mathrm{tip}}$, correspond to the negative elements of the Hessian matrix of $\mathcal{E}(\boldsymbol{\ell})$ that is evaluated for a particular fracture front configuration:

$$H_{\mathrm{s}ij} = -\frac{\partial^2 \mathcal{E}(\boldsymbol{\ell})}{\partial \ell_i \partial \ell_j} \tag{44}$$

$$H_{\mathrm{s}ij} = -\frac{\partial^2 \Pi(\boldsymbol{\ell})}{\partial \ell_i \partial \ell_j} + \frac{\partial G_{\mathrm{c}i}}{\partial \ell_j} \tag{45}$$

Since the analytical solution to the CCG problem (43) is generally difficult, a numerical approach will need to be applied instead. In order to solve the CCG problem efficiently,

a numerical scheme will have to be based around the particular shape (or curvature) of $\Psi(\boldsymbol{v})$ within the confines of the feasible solution space, as defined by the constraint conditions in (43). Within this solution space, $\Psi(\boldsymbol{v})$ can be downward-convex (concave), upward-convex (convex) or a generalised saddle function. These three behaviours of $\Psi(\boldsymbol{v})$ can be categorised as stable (41), unstable (40), and partially (un)stable (42) fracture front configurations respectively. In the vicinity of a feasible solution $\boldsymbol{v}$ the curvature of $\Psi(\boldsymbol{v})$ can be examined by assessing its second variation subject to $C(\boldsymbol{v}) = 0$:

$$\delta^2\Psi = H_{\mathrm{s}ij}\delta v_i \delta v_j \quad \forall \delta\boldsymbol{v} : \delta v_i \nabla C_i = 0, \tag{46}$$

where the gradient of $C(\boldsymbol{v})$ is a vector of ones. In (46), the equality-constraint reduces the available space of the variation $\delta\boldsymbol{v}$ by requiring that $\delta\boldsymbol{v}$ be orthogonal to the gradient of $C(\boldsymbol{v})$, i.e. $\delta v_i \nabla C_i = 0$. Therefore, the type of curvature that $\Psi(\boldsymbol{v})$ can exhibit along any feasible perturbation $\delta\boldsymbol{v}$ is determined by the definitiveness of the second order term $\delta^2\Psi(\mathbf{V}^*) = H_{\mathrm{s}ij}V_i^*V_j^*$ for all real-valued vectors $\mathbf{V}^*$ that satisfy $V_i^*\nabla C_i = 0$. To this end, $\mathbf{V}^*$ can be constructed from any same-dimension real-valued vector $\mathbf{V}$ by subtracting from $\mathbf{V}$ its projection in the direction of ∇C. In other words, $\mathbf{V}^*$ can be given as:

$$\mathbf{V}^* = \left(\mathbf{I} - \frac{\nabla C \nabla C^{\mathrm{T}}}{\nabla C^{\mathrm{T}} \nabla C}\right)\mathbf{V} \tag{47}$$

The definitiveness of $\delta^2\Psi(\mathbf{V}^*) = H_{\mathrm{s}ij}V_i^*V_j^*$, where $\mathbf{V}^*$ is constrained, can be effectively described in terms of that of $\delta^2\Psi^*(\mathbf{V}) = {H_{\mathrm{s}}^*}_{ij}V_iV_j$, where $\mathbf{V}$ is unconstrained and where the matrix H_{s}^* is the projection of H_{s} on the feasible solution plane; i.e., H_{s}^* is:

$$H_{\mathrm{s}}^* = \left(\mathbf{I} - \frac{\nabla C \nabla C^{\mathrm{T}}}{\nabla C^{\mathrm{T}} \nabla C}\right)^{\mathrm{T}} H_{\mathrm{s}} \left(\mathbf{I} - \frac{\nabla C \nabla C^{\mathrm{T}}}{\nabla C^{\mathrm{T}} \nabla C}\right) \tag{48}$$

It is remarked that the resulting symmetric matrix H_{s}^* is semidefinite because at least one eigenvalue is zero, e.g. $\nabla C_i {H_{\mathrm{s}}^*}_{ij} \nabla C_j = 0$. Nonetheless, the signs of the remaining eigenvalues of H_{s}^* can be used to characterise the relevant behaviour of $\Psi(\boldsymbol{v})$ within the feasible solution space. Therefore, $\Psi(\boldsymbol{v})$ is convex with respect to $\boldsymbol{v}$, subject to $C(\boldsymbol{v}) = 0$, if H_{s}^* is positive semidefinite (i.e. all the remaining eigenvalues of H_{s}^* are positive); $\Psi(\boldsymbol{v})$ is concave if H_{s}^* is negative semidefinite (i.e. the eigenvalues are negative); $\Psi(\boldsymbol{v})$ is a saddle function if H_{s}^* is indefinite (i.e. the eigenvalues are of mixed signs).

The stability property of the fracture front can be characterised using H_{s}^* in the same way. Thus, the fracture front is stable if H_{s}^* is negative semidefinite; the fracture front is unstable if H_{s}^* is positive semidefinite; the fracture front is partially (un)stable if H_{s}^* is indefinite. Figure 4 illustrates the usefulness of H_{s}^* in describing the relevant behaviour of $\Psi(\boldsymbol{v})$ for a few different instances involving a pair of competing crack tips.

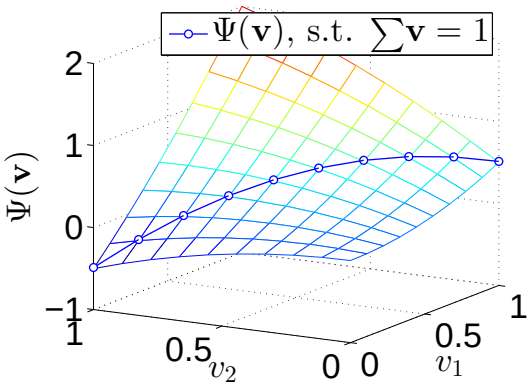

(a) H_s - indefinite;
H_s^* - negative semidefinite

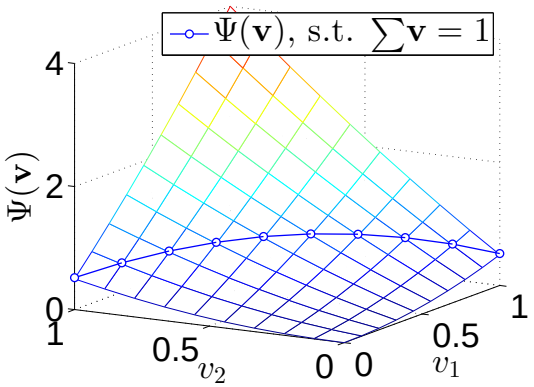

(b) H_s - positive definite;
H_s^* - negative semidefinite

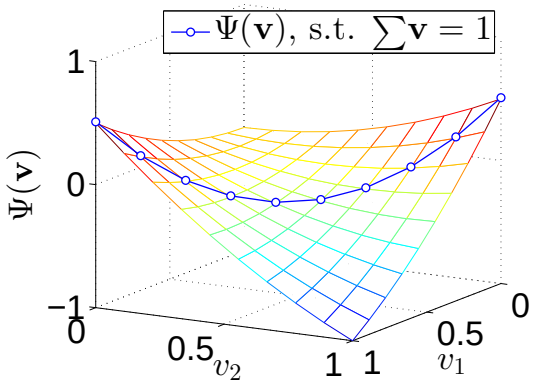

(c) H_s - indefinite;
H_s^* - positive semidefinite

Figure 4: Three instances of a pair of competing cracks, each showing a different shape of the objective function $\Psi(\boldsymbol{v})$ with its behaviour highlighted within the feasible solution space. The surface of $\Psi(\boldsymbol{v})$ is governed by H_s, whereas its behaviour within the feasible solution space is governed by H_s^*.

The following subsections delineate numerical solution methods for solving the competing crack growth problem (43) for arbitrary numbers of competing crack tips. The numerical solution methods are tailored to the stability property of the critical part of the fracture front (i.e. considering the critical crack tips). The solution methods are provided for the cases of: stable (41), unstable (40), and partially (un)stable (42) fracture fronts.

7.2.1 Fracture front is unstable

The simplest case arises when the critical fracture front is unstable (40). In this case, H_{s}^{*} is positive semidefinite by reason that it has no negative eigenvalues. The solution $\boldsymbol{v}$ that maximises $\Psi(\boldsymbol{v})$ can be determined by inspection of H_{s} alone; specifically, the solution is $v_i = 1$ where $i \in \mathcal{I}_{\mathrm{tip}}^{\mathrm{c}}$ is the tip that corresponds to the largest element on the diagonal of H_{s}. The particular case of competing crack growth is illustrated by Figure 4c.

Thus, under the conditions of an unstable fracture front configuration, only a single crack tip can advance since only then the growth maximises the objective function $\Psi(\boldsymbol{v})$. This has an important implication concerning symmetric problems where there are at least a few critical crack tips; specifically, it reveals that the symmetric fracture advance is unstable since an asymmetric solution (i.e. growth at one crack tip) is energetically favoured better over a symmetric solution. Case in point is the 2D problem of centre crack in a rectangular plate subjected to a vertical tensile load. For this problem, $H_{\mathrm{s}11} > H_{\mathrm{s}12}$ and, by symmetry, $H_{\mathrm{s}11} = H_{\mathrm{s}22}$ and $H_{\mathrm{s}12} = H_{\mathrm{s}21}$. The particular case is shown in Figure 4c. Firstly, by assuming a symmetric solution, i.e. $v_1 = v_2 = \frac{1}{2}$, the objective function acquires the value $\Psi_{\mathrm{sym}} = \frac{1}{8}(H_{\mathrm{s}11} + H_{\mathrm{s}22} + 2H_{\mathrm{s}12})$. On the other hand, by assuming an asymmetric solution, i.e. growth of one crack tip, gives $\Psi_{\mathrm{asym}} = \frac{1}{2}H_{\mathrm{s}11} = \frac{1}{2}H_{\mathrm{s}22}$. The difference in Ψ is $\Psi_{\mathrm{asym}} - \Psi_{\mathrm{sym}} \equiv \frac{1}{4}(H_{\mathrm{s}11} - H_{\mathrm{s}12}) > 0$. This indicates that the 2D problem favours an asymmetric solution, i.e. growth of one crack tip, rather than the symmetric solution, i.e. simultaneous growth of both crack tips.

7.2.2 Fracture front is stable

When the fracture front is stable (41), the matrix H_{s}^{*} is negative semidefinite, i.e. H_{s}^{*} has no positive eigenvalues. As a result, the function $\Psi(\boldsymbol{v})$ is concave (convex-down) within the feasible solution space. To find $\boldsymbol{v}$ that maximise $\Psi(\boldsymbol{v})$ (or that causes $\Psi(\boldsymbol{v})$ to decrease least) requires to solve the constrained quadratic optimisation problem (43). Since a closed-form solution is difficult by virtue of the imposed inequality constraints, a more practical approach is to apply an iterative solution scheme. One such technique that is well suited for handling inequality constrains is the active-set method for convex quadratic programming problems [80]. The method consists of first making a feasible guess for the initial solution (such that it satisfies all constraint conditions), then seeking to improve it in a series of equality-constrained optimizations. In more detail, the algorithm at iteration step k projects the current solution $\boldsymbol{v}^k$ for a set of active critical crack

tips $\mathcal{I}_{\text{tip}}^{\text{c},k} \subseteq \mathcal{I}_{\text{tip}}^{\text{c}}$ along a feasible direction $\boldsymbol{d}^k$ that maximises the objective function, subject to the equality constraints. The extent to which the solution is advanced along $\boldsymbol{d}^k$ is determined by a weight factor w^k such the objective function $\Psi^{k+1} = \Psi(\boldsymbol{v}^k + w^k \boldsymbol{d}^k)$ is either maximised locally (i.e. reaches an extremum) or it is maximised up to a point the solution hits any of the inequality constrains. When it is the latter case, the subsequent iteration $k+1$ treats the about-to-fail inequality constraint as an equality constraint. This effectively leads to consider a reduced set of critical crack tips $\mathcal{I}_{\text{tip}}^{\text{c},k+1} = \mathcal{I}_{\text{tip}}^{\text{c},k} \backslash i$.

Since the inequality constraints act only as bounds that limit the advance of solution $\boldsymbol{v}^k$ to maximise Ψ^{k+1}, the optimal advance direction $\boldsymbol{d}^k = \boldsymbol{v}^{k+1} - \boldsymbol{v}^k$ can be determined by using the method of Lagrangian multipliers because the problem at hand is effectively an equality-constrained optimisation. The Lagrangian at iteration time k reads:

$$\mathcal{L}(\boldsymbol{v}^{k+1}, \lambda^{k+1}) = \frac{1}{2} H_{\text{s}ij}\, v_i^{k+1} v_j^{k+1} + \lambda^{k+1}(\mathbf{e}_i v_i^{k+1} - 1), \quad \text{for } i,j \in \mathcal{I}_{\text{tip}}^{\text{c},k} \tag{49}$$

The solution to $\{\boldsymbol{v}^{k+1}, \lambda^{k+1}\}$ corresponds to the stationary point of the Lagrangian. Taking the variation of $\mathcal{L}(\boldsymbol{v}^{k+1}, \lambda^{k+1})$ with respect to each variable in turn yields:

$$H_{\text{s}ij} v_j^{k+1} + \mathbf{e}_i \lambda^{k+1} = 0 \tag{50}$$

$$\mathbf{e}_i v_i^{k+1} - 1 = 0 \tag{51}$$

Solving (50) and (51) gives the solution to the *idealised* rate of fracture advance, $\boldsymbol{v}^{k+1}$. The solution $\boldsymbol{v}^{k+1}$ is termed *idealised* because the requirement for a strictly non-negative solution is unenforced. Nonetheless, the solution advance direction $\boldsymbol{d}^k = \boldsymbol{v}^{k+1} - \boldsymbol{v}^k$ at iteration step k can be used. In this case, $\boldsymbol{d}^k$ take the following form:

$$d_i^k = \frac{{H_{\text{s}}^{-1}}_{ij}\, \mathbf{e}_j}{{H_{\text{s}}^{-1}}_{ij}\, \mathbf{e}_i\, \mathbf{e}_j} - v_i^k \quad \text{for } i \in \mathcal{I}_{\text{tip}}^{\text{c},k} \tag{52}$$

The amount that the solution $\boldsymbol{v}^k$ can advanced along the direction $\boldsymbol{d}^k$ is determined by the weight-factor $w^k \in [0,1]$ such that an improved solution is $\boldsymbol{v}^{k+1} = \boldsymbol{v}^k + w^k \boldsymbol{d}^k$. The weight factor w^k is computed based on the distance from the current solution $\boldsymbol{v}^k$ to the most imminent boundary of any inequality constraint such that $v_i^{k+1} \geq 0\ \forall i \in \mathcal{I}_{\text{tip}}^{\text{c},k}$. This leads to the following expression for the maximum (positive) value of the weight:

$$w^k = \min\left(\frac{v_i^k}{-d_i^k}, 1\right) \quad \text{where } i \in \mathcal{I}_{\text{tip}}^{\text{c},k} \tag{53}$$

A pseudo-code of the algorithm for solving the competing crack growth problem (43) for the specific case of a stable fracture front is provided in Appendix B.

7.2.3 Fracture front is partially stable

For the general case of a partially stable fracture front (42), the matrix H_{s}^{*} is indefinite, i.e. H_{s}^{*} has eigenvalues of mixed signs. As a result, the function $\Psi(\boldsymbol{v})$ behaves as a generalised saddle function within the feasible solution space. This, in turn, prevents the two previously delineated techniques from being used effectively since they are limited to convex problems only. The non-convexity of $\Psi(\boldsymbol{v})$ gives rise to a solution space that can contain many extrema, among which it can prove difficult to determine the solution that globally maximises $\Psi(\boldsymbol{v})$. For this reason it may be necessary to examine all stationary solutions as well as the solutions that lie on the vertices of the feasible domain. In order to solve the CCG problem (43) for this case, we adopt a gradient-descent solution method. Specifically, the solution advance direction is determined as the projection of the gradient of $\Psi(\boldsymbol{v})$ on the plane that is orthogonal to ∇C. The solution $\boldsymbol{v}^k$ at iteration step k is advanced following the active-set framework, as described previously; however, any chance of downward convexity of Ψ along a particular solution advance directions is exploited. In this formulation, the solution advance vector $\boldsymbol{d}^k$ is obtained as:

$$d_i^k = \left(\delta_{ij} - \frac{\nabla C_i \, \nabla C_j}{\nabla C_q \nabla C_q}\right) \nabla \Psi_j^k \quad \text{where } i, j, q \in \mathcal{I}_{\mathrm{tip}}^{\mathrm{c},k} \tag{54}$$

where the gradient of the objective function is $\nabla \Psi_i^k = H_{\mathrm{s}ij} \, v_j^k$. Since the gradient of the equality constraint is a vector of ones, i.e. $\nabla C = \mathbf{1}$, equation (54) simplifies to:

$$d_i^k = \nabla \Psi_i^k - \mathrm{mean}(\nabla \Psi^k) \tag{55}$$

The solution is projected along $\boldsymbol{d}^k$ using the weight factor $w^k \geq 0$ to the extent that no inequality constraint is violated, i.e. $v_i^{k+1} = v_i^k + w^k d_i^k \geq 0$ for $i \in \mathcal{I}_{\mathrm{tip}}^{\mathrm{c},k}$. Thus, w^k is similar to that in (53), though the upper-limit can be omitted so long as $\Psi(\boldsymbol{v}^k + w^k \boldsymbol{d}^k)$ is upward-convex with respect to w^k, i.e. $H_{\mathrm{s}ij} d_i^k d_j^k > 0$. The expression for w^k reads:

$$w^k = \min\left(\frac{v_i^k}{-d_i^k}\right) \quad \text{where } i \in \mathcal{I}_{\mathrm{tip}}^{\mathrm{c},k} \tag{56}$$

In case $\Psi(\boldsymbol{v}^k + w^k \boldsymbol{d}^k)$ is downward-convex with respect to w^k, i.e. $H_{\mathrm{s}ij} d_i^k d_j^k < 0$, an optimum weight factor w^k can be determined via a line-search technique. The locally optimal value of the weight factor w^k is obtained by solving for the stationarity value of $\Psi(\boldsymbol{v}^k + w^k \boldsymbol{d}^k)$ with respect to w^k while minding the inequality constrains via (56):

$$w^k = -\frac{H_{\mathrm{s}ij} d_i^k v_j^k}{H_{\mathrm{s}ij} d_i^k d_j^k} \text{ provided } H_{\mathrm{s}ij} d_i^k d_j^k < 0 \text{ and} \tag{57}$$
$$\text{subject to } w^k < \min\left(\frac{v_i^k}{-d_i^k}\right) \text{ where } i,j \in \mathcal{I}_{\mathrm{tip}}^{\mathrm{c},k}$$

Note that the converged solution $\boldsymbol{v}^n$ (when $n \to \infty$) can depend on the initial (trial) solution $\boldsymbol{v}^0$. For this reason, it is generally required to assess different starting points, e.g. the vertices of the feasible solution space, in order to find the globally optimal solution. A pseudo-code of the algorithm for solving the competing crack growth problem (43) for the general case of a partially (un)stable fracture front is provided in Appendix C.

7.3 Comparison to previous work

Below is a diagrammatic summary of the proposed solution strategies for resolving competing crack growth based on the stability of the fracture front configuration (30).

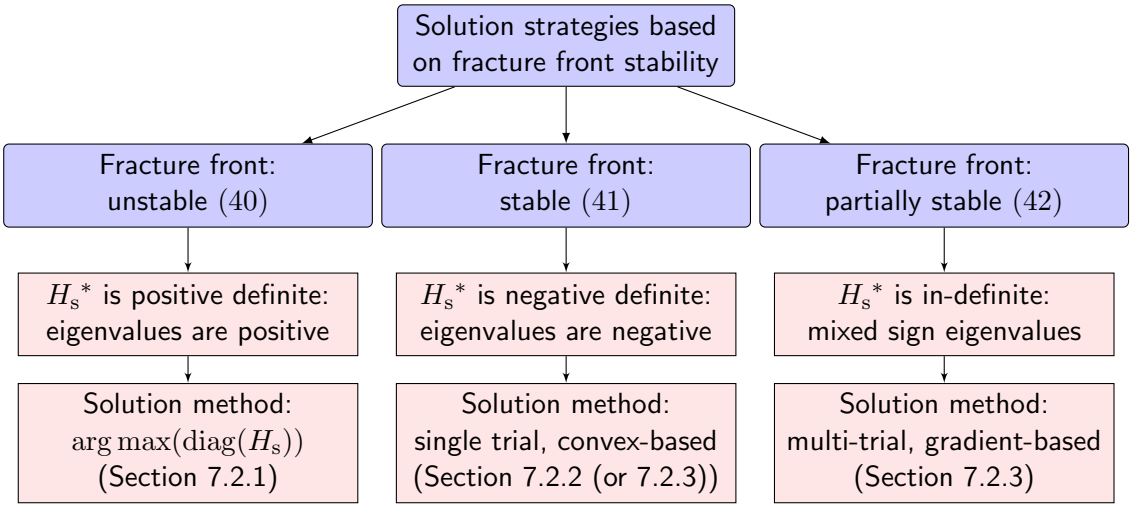

Figure 5: Choice of solution strategy to the problem of competing crack growth based on the stability of the competing crack tip configuration.

Reference [17] that dealt with multi-crack growth within the LEFM framework also considered the problem of competing crack growth. At the instance of crack tip competition (e.g. when the equivalent stress intensity factors at several crack tips approach critical values) a *stability analysis* [17] is performed to determine the active competing crack tips that should be extended. This involves evaluating all possible sub-determinants of the matrix of the rates of the energy release rates (36) and growing the subset of the

competing crack tips that corresponds to the maximum sub-determinant. When the maximum sub-determinant is positive, the tip configuration is said to be *unstable* and the active crack tips are obtained directly. If the maximum sub-determinant is negative, the tip configuration is said to be *stable*; in this case, the solution is one that dissipates the least energy. In either case, each active crack tip is extended by a constant increment in the direction given by the maximum hoop stress criterion [23].

Our approach is different in that we seek the crack tip extension configuration that dissipates the most energy per unit fracture area increase (regardless of the type of stability of the competing crack tips); therefore, the maximum sub-determinant [17] and our total energy minimisation approach will generally yield differ solutions. To show this, several fabricated example cases of stable, unstable and partially stable competing crack tip configurations are analysed in Appendix A. Our approach is also different from [17] in that we determine the crack tip extension directions based on the maximum energy dissipation principle, which stems directly from Griffith's law (22), instead of using the rather heuristic maximum hoop stress criterion, which is the case in [17].

The following section provides the detailed derivation of the crack growth direction criterion that is consistent with the maximum energy dissipation principle.

8 Direction of crack growth

In a 2D framework, the incipient growth direction of any crack tip $i \in \mathcal{I}_{\text{tip}}$ can be specified in terms of the crack tip growth angle θ_i or in terms of the crack tip kink angle $\Delta\theta_i$. If $\delta\boldsymbol{\ell} \in \mathbb{R}^n_{>0}$ consists of n small crack tip extensions, i.e. $\delta\ell_i \to 0^+ \ \forall i \in \mathcal{I}_{\text{tip}}$, then minimising the total energy $\mathcal{E}(\delta\boldsymbol{\ell}, \Delta\boldsymbol{\theta})$ with respect to $\Delta\boldsymbol{\theta}$ is equivalent to finding $\Delta\boldsymbol{\theta}$ that maximises the incipient energy dissipation rate $\mathcal{D}(\boldsymbol{\ell}, \Delta\boldsymbol{\theta}) \equiv \mathcal{D}_i(\boldsymbol{\ell}, \Delta\theta_i)\hat{\ell}_i$. In order for $\mathcal{D}(\boldsymbol{\ell}, \Delta\boldsymbol{\theta})$ to be maximum, the individual crack tip energy dissipation rates $\mathcal{D}_i(\boldsymbol{\ell}, \Delta\theta_i)$ must be maximum, regardless of the relative crack tip growth rates ($\hat{\ell}_i = \mathrm{d}\ell_i/\mathrm{d}a$). Thus, each crack tip $i \in \mathcal{I}_{\text{tip}}$ has a preferred growth direction that locally maximises $\mathcal{D}_i(\theta_i)$. The optimality condition for θ_i, in the sense of a maximum $\mathcal{D}_i(\theta_i)$, can be written as:

$$\frac{\mathrm{d}\mathcal{D}_i}{\mathrm{d}\theta_i} = 0, \text{ assuming } \frac{\mathrm{d}^2\mathcal{D}_i}{\mathrm{d}^2\theta_i} < 0 \tag{58}$$

Alternatively, (58) can be expressed as a stationary total energy $\mathcal{E}\big(\Delta\ell_i, \theta_i\big)$ with respect to the sweeping crack tip extension $\Delta\ell_i > 0$ through the angle θ_i in the limit the extension tends to zero, i.e. $\Delta\ell_i \to 0^+$. The alternative form is obtained from (58) by integrating $\mathcal{D}_i = -\mathrm{d}\mathcal{E}/\mathrm{d}\ell_i$ with respect to ℓ_i over the infinitesimal crack tip extension $\Delta\ell_i$:

$$\lim_{\Delta\ell_i \to 0^+} \left(-\frac{\mathrm{d}\mathcal{E}}{\mathrm{d}\theta_i}\bigg|_{\Delta\ell_i} \right) = 0, \text{ assuming } \lim_{\Delta\ell_i \to 0^+} \left(-\frac{\mathrm{d}^2\mathcal{E}}{\mathrm{d}\theta_i^2}\bigg|_{\Delta\ell_i} \right) < 0 \tag{59}$$

For the purposes of notational convenience, $\mathcal{D}_{\theta i}$ is introduced to represent the average rotational dissipation of the fracture extension $\Delta\ell_i$ with respect to its angle θ_i:

$$\mathcal{D}_{\theta i} = -\frac{\mathrm{d}\mathcal{E}}{\mathrm{d}\theta_i}\bigg|_{\Delta\ell_i} \tag{60}$$

The rotational dissipation term $\mathcal{D}_{\theta i}$ describes how the total energy $\mathcal{E}$ of the mechanical system changes with respect to the rotation of the crack tip extension $\Delta\ell_i$ in terms of its angle θ_i. Substituting (60) in (59) gives the criterion for the incipient crack growth angle θ_i in terms of the fracture state of zero rotational dissipation:

$$\lim_{\Delta\ell_i\to 0^+} \mathcal{D}_{\theta i} = 0, \text{ subject to } \lim_{\Delta\ell_i\to 0^+} \left(\frac{\mathrm{d}\mathcal{D}_{\theta i}}{\mathrm{d}\theta_i}\right) < 0, \tag{61}$$

Provided the crack tip increments are sufficiently small, their mutual interactions become negligible; hence, the optimality of θ_i via the condition $\mathcal{D}_{\theta i} = 0$ is asserted by determining that $\mathrm{d}\mathcal{D}_{\theta i}/\mathrm{d}\theta_i < 0$ is satisfied $\forall i \in \mathcal{I}_{\text{tip}}$. The main advantage of (61) to determining the crack tip extension directions over the maximum dissipation principle (58) is that the former is readily extendable to finite crack increments, i.e. a discrete framework.

9 Conclusions

The first part of our three-part paper has focused on the theory of crack evolution under quasi-static conditions in an isotropic linear-elastic solid based on the principle of minimum total energy (30), which stems directly from the Griffith's law of crack growth (22). The benefit of the minimum energy approach is that the time-continuous minimisation of the energy functional naturally leads to the evolution of the displacement field satisfying static equilibrium and to the evolution of the fracture surfaces satisfying energy conservation and Griffith's law. Although the energy minimal solution is more difficult to determine at the instance of competing crack growth, three solution strategies were proposed according to the type of stability of the crack tip configuration at hand. Subsequently, the crack growth direction law based on the minimum energy principle (59) was formulated as the criterion of vanishing rotational dissipation rates (61) of the crack tip extensions. The particular advantage of the formulation (61) is that it can be easily applied within a discrete framework involving finite-length crack tip increments.

Our solution approach is different from that in reference [17] in two major ways. Firstly, we have shown by giving concrete examples that the maximum sub-determinant method used in [17] is generally not equivalent to the minimum energy solution. Secondly, in reference [17], the crack growth directions are determined using the maximum stress criterion, which is not consistent with Griffith's law under mixed-mode loading.

Part-I of our three-part paper has mainly served as a stepping stone for applying the energy minimisation techniques within a discrete context using a discretisation of choice (e.g. the extended finite element method). Our approach to determining which cracks grow, in what directions and when just by minimising the total energy functional is attractive as it is not necessary to rely on the precise crack tip field characterisation (e.g. compute SIFs) nor resort to heuristic criteria (e.g. the maximum hoop-stress or other criteria that are based on SIFs) as our approach is consistent with Griffith's law. For this reason, the minimum energy approach is generally applicable to problems involving spatially varying material toughness and for non-remote loading conditions (e.g. body loads, residual strains/stresses, crack surface tractions) where the application of other classic criteria are not so easy to justify. Our following paper, Part-II, deals with the discrete framework and applies the fracture governing principles within XFEM.

10 Supplementary material

The open-source code XFEM_Fracture2D and supporting material can be found here:

- XFEM_Fracture2D: https://figshare.com/s/0b4394e8fab7191d2692
- competing cracks: https://figshare.com/s/4a7dd5fb0a8634c9fae4
- demo screenshots: https://figshare.com/s/6397737c78beb59f3b58
- demo movies: https://figshare.com/s/73d7b50a7729070c2173

A Comparison of competing crack growth solutions: maximum sub-determinant vs. maximum dissipation

We show that the maximum subdeterminant and the maximum energy dissipation criteria are generally not equivalent in cases of more than two competing crack tips. This is done with the help of a few fabricated case studies; specifically, we consider the possible scenarios of competing crack growth: (1) unstable, (2) stable, and (3) partially stable crack tip configurations. For each scenario we illustrate a possible case where the solutions by the two criteria are different. The solutions are compared in terms of the average energy dissipation rate:

$$\bar{G}_{\mathrm{s}} = -\frac{\delta\Pi}{\delta a} = G_{\mathrm{s}0} + \frac{1}{2} H_{\mathrm{s}ij} \frac{\delta \ell_i}{\delta a} \frac{\delta \ell_j}{\delta a} \delta a, \tag{62}$$

where $G_{\mathrm{s}0}$ is the value of energy release rate at each of the competing crack tips prior to crack growth, $H_{\mathrm{s}ij} \equiv \partial G_{\mathrm{s}i}/\partial \ell_j$ are the rates of the energy release rates, and δa is a small increase in the fracture area.

A.1 Unstable competing crack growth

Consider the following example case of an unstable crack tip configuration (i.e. the matrix of the rates of the energy release rates is positive definite):

$$H_{\mathrm{s}ij} \equiv \partial G_i/\partial \ell_j = \begin{bmatrix} 1 & 1 & 1 \\ 1 & 2 & 1 \\ 1 & 1 & 3 \end{bmatrix} \tag{63}$$

The maximum sub-determinant of the matrix H_{s} is 5. The solution directly corresponds to the growth of the 2$^{\mathrm{nd}}$ and 3$^{\mathrm{rd}}$ crack tips since the sub-determinant is positive. According to [17], the two crack tips advance at the same rate $\delta\ell/\delta a = [0, 0.5, 0.5]$. On the other hand, the maximum dissipation solution is $\delta\ell/\delta a = [0, 0, 1]$. The solutions correspond to these energy dissipation rates: $\bar{G}_{\mathrm{smaxsubdet}} = G_{\mathrm{s}0} + 0.8750\,\delta a$ and $\bar{G}_{\mathrm{smaxdissip}} = G_{\mathrm{s}0} + 1.5\,\delta a$ respectively. Thus, the maximum sub-determinant solution gives a lower rate of energy dissipation for a given external load application for an arbitrarily small δa. Consequently, the maximum sub-determinant solution is less energetically favourable from the point of view of Griffith's crack growth criterion.

A.2 Stable competing crack growth

Consider a case where the crack tip configuration is stable (i.e. the matrix of the rates of the energy release rates is negative definite):

$$H_{\mathrm{s}} = -\begin{bmatrix} 1 & 1 & 1 \\ 1 & 2 & 1 \\ 1 & 1 & 3 \end{bmatrix} \tag{64}$$

The maximum sub-determinate of the matrix H_{s} is 5 (same as in the previous case). According to [17] the active crack tips are given directly and the crack tip advance solution is $\delta\ell/\delta a = [0, 0.5, 0.5]$. On the other hand, the maximum dissipation solution is $\delta\ell/\delta a = [1, 0, 0]$. These solutions correspond to energy dissipation rates of $\bar{G}_{\mathrm{smaxsubdet}} = G_{\mathrm{s0}} - 0.8750\,\delta a$ and $\bar{G}_{\mathrm{smaxdissip}} = G_{\mathrm{s0}} - 0.5\,\delta a$ respectively. Thus, the maximum sub-determinant solution is again sub-optimal from the viewpoint of Griffith.

A.3 Partially stable competing crack growth

Finally, consider a case where the crack tip configuration is only partially stable (i.e. the matrix of the rates of the energy release rates is indefinite):

$$H_{\mathrm{s}} = \begin{bmatrix} -1 & 1 & 1 \\ 1 & 2 & 1 \\ 1 & 1 & -1 \end{bmatrix} \tag{65}$$

The maximum sub-determinant of H_{s} is 4. Since the sub-determinant is positive, the solution is given directly as $\delta\ell/\delta a = [1/3, 1/3, 1/3]$. The maximum dissipation solution is $\delta\ell/\delta a = [0, 1, 0]$. These solutions correspond to mean energy dissipation rates of $\bar{G}_{\mathrm{smaxsubdet}} = G_{\mathrm{s0}}{+}1/3\,\delta a$ and $\bar{G}_{\mathrm{smaxsubdet}} = G_{\mathrm{s0}}{+}1\,\delta a$ respectively. Thus, the maximum sub-determinant solution is energetically sub-optimal.

B Competing crack growth solution algorithm for a strictly stable fracture front

Algorithm 1 Compute $a = \arg\max_{v \in \mathcal{A}} \left(\frac{1}{2} v^{\mathrm{T}} H_s v\right)$,
subject to the constraints: $\|a\|_1 - 1 = 0$ and $a_i \geq 0$, and
where $H_s^* = \left(I - \frac{\mathbf{e}^{\mathrm{T}}\mathbf{e}}{\mathbf{e}\,\mathbf{e}^{\mathrm{T}}}\right) H_s \left(I - \frac{\mathbf{e}^{\mathrm{T}}\mathbf{e}}{\mathbf{e}\,\mathbf{e}^{\mathrm{T}}}\right)$ is negative semidefinite.

Require: $\sum a_i = 1$ and $a_i \geq 0$ for $i \in \mathcal{I}_{\mathrm{crit}}$ {feasible initial guess}
  $n \leftarrow |\mathcal{I}_{\mathrm{crit}}|$ {get size of set of critical crack tips}
  $d \leftarrow \mathrm{zeros}(n, 1)$ {initialize fracture advance direction}
  $e \leftarrow \mathrm{ones}(n, 1)$ {gradient of the equality-constraint equation}
  $p \leftarrow \mathrm{true}(n, 1)$ {logical form of the working set}
  while 1 **do**
    $a_0 \leftarrow a$ {store current solution as reference}
    while 1 **do**
      $d[p] \leftarrow \frac{H_s[p,p]^{-1} e[p]}{e[p]^{\mathrm{T}} H_s[p,p]^{-1} e[p]} - a[p]$ {trial advance satisfying $\sum_{i=1}^{n} d[i] = 0$}
      $q \leftarrow \mathrm{and}(d < 0, a < \mathrm{tol})$ {get infeasible points}
      if $\mathrm{any}(q = \mathbf{true})$ **then**
        $d[q] \leftarrow 0$ {discard all infeasible points}
        $p[q] \leftarrow 0$ {update working set}
      else
        break {working set is feasible}
      end if
    end while
    $q \leftarrow \mathrm{and}(d < 0, a > 0)$ {get imminent constraints}
    $w \leftarrow \min\left(\left\{\frac{a[q]}{-d[q]}, 1\right\}\right)$ {projection weight factor}
    $a \leftarrow a + wd$ {update previous solution}
    if $\mathrm{or}(1 - w < \mathrm{tol}, \|a - a_0\| < \mathrm{tol})$ **then**
      break {solution converged}
    end if
  end while
  return a

C Competing crack growth solution algorithm for a partially (un)stable fracture front

Algorithm 2 Compute $a = \arg\max_{v \in \mathcal{A}} \left(\frac{1}{2} v^{\mathrm{T}} H_s v\right)$,
subject to the constraints: $\|a\|_1 - 1 = 0$ and $a_i \geq 0$, and
where $H_s^* = \left(I - \frac{\mathbf{e}^{\mathrm{T}}\mathbf{e}}{\mathbf{e}\,\mathbf{e}^{\mathrm{T}}}\right) H_s \left(I - \frac{\mathbf{e}^{\mathrm{T}}\mathbf{e}}{\mathbf{e}\,\mathbf{e}^{\mathrm{T}}}\right)$ is positive semidefinite.

Require: $\sum a_i = 1$ and $a_i \geq 0$ for $i \in \mathcal{I}_{\mathrm{crit}}$ {feasible initial guess}
  $n \leftarrow |\mathcal{I}_{\mathrm{crit}}|$ {get size of set of critical crack tips}
  $e \leftarrow \mathrm{ones}(n, 1)$ {gradient of the equality-constraint}
  $a_{\mathrm{all}} \leftarrow \mathrm{zeros}(n, n)$ {for storing all converged solutions}
  $\Psi_{\mathrm{all}} \leftarrow \mathrm{zeros}(n, 1)$ {for storing objective function values}
  for $i = 1$ **to** n **do**
    $a \leftarrow \mathrm{zeros}(n, 1)$
    $a[i] \leftarrow 1$ {trial}
    while 1 **do**
      $a_0 \leftarrow a$ {store current solution as reference}
      $g \leftarrow H_s a$ {gradient of the objective function}
      $d \leftarrow \mathrm{zeros}(n, 1)$ {initialize fracture advance vector}
      $p \leftarrow \mathrm{true}(n, 1)$ {logical form of the working set}
      while 1 **do**
        $d[p] \leftarrow g[p] - \mathrm{mean}(g[p])$ {steepest gradient advance satisfying $\sum_{i=1}^{n} d[i] = 0$}
        $q \leftarrow \mathrm{and}(d < 0, a < \mathrm{tol})$ {get infeasible points}
        if $\mathrm{any}(q = \mathbf{true})$ **then**
          $d[q] \leftarrow 0$ {discard all infeasible points}
          $p[q] \leftarrow 0$ {update working set}
        else
          break {working set is feasible}
        end if
      end while
      $q \leftarrow \mathrm{and}(d < 0, a > 0)$ {get imminent constraints}
      $w \leftarrow \min\left(\left\{\frac{a[q]}{-d[q]}\right\}\right)$ {projection weight factor}
      if $d^{\mathrm{T}} H_s d < 0$ **then**
        {objective function is concave along d as projected from a}
        $w \leftarrow \min\left(w, \frac{d^{\mathrm{T}} H_s a}{d^{\mathrm{T}} H_s d}\right)$ {use the optimum weight factor if possible}
      end if
      $a \leftarrow a + wd$ {update previous solution}
      if $\|a - a_0\| < \mathrm{tol}$ **then**
        break {solution converged}
      end if
    end while
    $a_{\mathrm{all}}[:, i] \leftarrow a$
    $\Psi_{\mathrm{all}}[i] \leftarrow \frac{1}{2} a^{\mathrm{T}} H_s a$
  end for
  $i_{\max} \leftarrow \mathrm{find}(\Psi = \max(\Psi_{\mathrm{all}}))$
  return $a \leftarrow a_{\mathrm{all}}[:, i_{\max}]$

References

[1] M. Ambati, T. Gerasimov, and L. De Lorenzis. "A review on phase-field models of brittle fracture and a new fast hybrid formulation". In: *Computational Mechanics* 55.2 (2015), pp. 383–405. ISSN: 0178-7675.

[2] T. L. Anderson. *Fracture Mechanics: Fundamentals and Applications*. Third Edit. Boca Raton: CRC Press, 2005. ISBN: 978-1-4200-5821-5.

[3] M. P. Areias and T. Belytschko. "Analysis of three-dimensional crack initiation and propagation using the extended finite element method". In: *International Journal for Numerical Methods in Engineering* 63.5 (2005), pp. 760–788. ISSN: 0029-5981.

[4] G. Baker. "Thermodynamics in solid mechanics: a commentary". In: *Philosophical Transactions of the Royal Society A: Mathematical, Physical and Engineering Sciences* 363.1836 (2005), pp. 2465–2477. ISSN: 1364-503X.

[5] P. F. Becher. "Microstructural Design of Toughened Ceramics". In: *Journal of the American Ceramic Society* 74.2 (1991), pp. 255–269. ISSN: 0002-7820.

[6] T. Belytschko and S. P. Xiao. "Coupling Methods for Continuum Model with Molecular Model". In: *International Journal for Multiscale Computational Engineering* 1.1 (2003), p. 12. ISSN: 1543-1649.

[7] E. Benvenuti, A. Tralli, and G. Ventura. "A regularized XFEM model for the transition from continuous to discontinuous displacements". In: *International Journal for Numerical Methods in Engineering* 74.6 (2008), pp. 911–944. ISSN: 00295981.

[8] P. Bernard, N. Moës, and N. Chevaugeon. "Damage growth modeling using the Thick Level Set (TLS) approach: Efficient discretization for quasi-static loadings". In: *Computer Methods in Applied Mechanics and Engineering* 233-236 (2012), pp. 11–27. ISSN: 00457825.

[9] S. Bordas, T. Rabczuk, and G. Zi. "Three-dimensional crack initiation, propagation, branching and junction in non-linear materials by an extended meshfree method without asymptotic enrichment". In: *Engineering Fracture Mechanics* 75.5 (2008), pp. 943–960. ISSN: 00137944.

[10] S. P. A. Bordas and B. Moran. "Enriched finite elements and level sets for damage tolerance assessment of complex structures". In: *Engineering Fracture Mechanics* 73.9 (2006), pp. 1176–1201. ISSN: 00137944.

[11] M. J. Borden et al. "A phase-field description of dynamic brittle fracture". In: *Computer Methods in Applied Mechanics and Engineering* 217-220.2012 (2012), pp. 77–95. ISSN: 00457825.

[12] P. Bouchard, F. Bay, and Y. Chastel. "Numerical modelling of crack propagation: automatic remeshing and comparison of different criteria". In: *Computer Methods in Applied Mechanics and Engineering* 192.35-36 (2003), pp. 3887–3908. ISSN: 00457825.

[13] B. Bourdin, G. A. Francfort, and J. J. Marigo. "Numerical experiments in revisited brittle fracture". In: *Journal of the Mechanics and Physics of Solids* 48.4 (2000), pp. 797–826. ISSN: 00225096.

[14] B. Bourdin, G. A. Francfort, and J. J. Marigo. "The Variational Approach to Fracture". In: *Journal of Elasticity* 91.1-3 (2008), pp. 5–148. ISSN: 0374-3535.

[15] W. F. Brace and E. G. Bombolakis. "A note on brittle crack growth in compression". In: *Journal of Geophysical Research* 68.12 (1963), pp. 3709–3713. ISSN: 01480227.

[16] P. R. Budarapu et al. "Efficient coarse graining in multiscale modeling of fracture". In: *Theoretical and Applied Fracture Mechanics* 69 (2014), pp. 126–143. ISSN: 01678442.

[17] E. Budyn et al. "A method for multiple crack growth in brittle materials without remeshing". In: *International Journal for Numerical Methods in Engineering* 61.10 (2004), pp. 1741–1770. ISSN: 0029-5981.

[18] M. Buliga. "Energy Minimization Brittle Crack Propagation". In: *Journal of Elasticity* 52.3 (1998), pp. 201–238. ISSN: 03743535.

[19] H. Courtecuisse et al. "Real-time simulation of contact and cutting of heterogeneous soft-tissues". In: *Medical Image Analysis* 18.2 (2014), pp. 394–410. ISSN: 13618415.

[20] G. Del Piero, G. Lancioni, and R. March. "A variational model for fracture mechanics: Numerical experiments". In: *Journal of the Mechanics and Physics of Solids* 55.12 (2007), pp. 2513–2537. ISSN: 00225096.

[21] R. Denys et al. *Report of the National Scientific Expert Group on the RPVD3T2.* Tech. rep. January. The National Scientific Exper Group, 2013, pp. 1–14.

[22] P. Dumstorff and G. Meschke. "Crack propagation criteria in the framework of X-FEM-based structural analyses". In: *International Journal for Numerical and Analytical Methods in Geomechanics* 31.2 (2007), pp. 239–259. ISSN: 03639061.

[23] F. Erdogan and G. C. Sih. "On the Crack Extension in Plates Under Plane Loading and Transverse Shear". In: *Journal of Basic Engineering* 85.4 (1963), p. 519. ISSN: 00219223.

[24] A. G. Evans and K. T. Faber. "Toughening of Ceramics by Circumferential Microcracking". In: *Journal of the American Ceramic Society* 64.7 (1981), pp. 394–398. ISSN: 0002-7820.

[25] A. Evans and Y. Fu. "Some effects of microcracks on the mechanical properties of brittle solidsII. Microcrack toughening". In: *Acta Metallurgica* 33.8 (1985), pp. 1525–1531. ISSN: 00016160.

[26] A. G. Evans. "Perspective on the Development of High-Toughness Ceramics". In: *Journal of the American Ceramic Society* 73.2 (1990), pp. 187–206. ISSN: 0002-7820.

[27] F. Fantoni. "Fracture growth in brittle and embrittled materials: variational formulations and crack tracking algorithms". Mathematical Methods and Models for Engineering. Universita Degli Studi Di Brescia, 2016.

[28] X. Q. Feng and Y. Huang. "Mechanics of Smart-Cut® technology". In: *International Journal of Solids and Structures* 41.16-17 (2004), pp. 4299–4320. ISSN: 00207683.

[29] X. Q. Feng et al. “Fracture mechanics analysis of three-dimensional ion cut technology”. In: *Journal of Mechanics of Materials and Structures* 2.9 (2007), pp. 1831–1852. ISSN: 1559-3959.

[30] G. Francfort and J.-J. Marigo. “Revisiting brittle fracture as an energy minimization problem”. In: *Journal of the Mechanics and Physics of Solids* 46.8 (1998), pp. 1319–1342. ISSN: 00225096.

[31] G. A. Francfort and A. Garroni. “A Variational View of Partial Brittle Damage Evolution”. In: *Archive for Rational Mechanics and Analysis* 182.1 (2006), pp. 125–152. ISSN: 0003-9527.

[32] M. Frémond and B. Nedjar. “Damage, gradient of damage and principle of virtual power”. In: *International Journal of Solids and Structures* 33.8 (1996), pp. 1083–1103. ISSN: 00207683.

[33] A. Giacomini. “Ambrosio-Tortorelli approximation of quasi-static evolution of brittle fractures”. In: *Calculus of Variations* 22.2 (2005), pp. 129–172. ISSN: 0944-2669. arXiv: `0303040 [math]`.

[34] R. V. Gol’dstein and R. L. Salganik. “Brittle fracture of solids with arbitrary cracks”. In: *International Journal of Fracture* 10.4 (1974), pp. 507–523. ISSN: 03769429.

[35] A. A. Griffith. “The Phenomena of Rupture and Flow in Solids”. In: *Philosophical Transactions of the Royal Society of London* A221 (1920), pp. 163–198.

[36] A. A. Griffith. “The Phenomena of Rupture and Flow in Solids”. In: *Philosophical Transactions of the Royal Society of London. Series A, Containing Papers of a Mathematical or Physical Character* 221 (1921), pp. 163–198.

[37] B. Gu et al. “Fracture mechanics analysis on Smart-Cut® technology. Part 1: Effects of stiffening wafer and defect interaction”. In: *Acta Mechanica Sinica* 25.1 (2009), pp. 73–81. ISSN: 0567-7718.

[38] B. Gu et al. “Fracture mechanics analysis on Smart-Cut® technology. Part 2: Effect of bonding flaws”. In: *Acta Mechanica Sinica* 25.2 (2009), pp. 197–203. ISSN: 0567-7718.

[39] E. Gürses. “Aspects of Energy Minimization in Solid Mechanics : Evolution of Inelastic Microstructures and Crack Propagation”. PhD thesis. 2007. ISBN: 3937859071.

[40] K. Hayashi and S. Nemat-Nasser. “Energy-Release Rate and Crack Kinking Under Combined Loading”. In: *Journal of Applied Mechanics* 48.3 (1981), p. 520. ISSN: 00218936.

[41] J. A. Hodgdon and J. P. Sethna. “Derivation of a general three-dimensional crack-propagation law: A generalization of the principle of local symmetry”. In: 47.9 (1993).

[42] J. Hou et al. *An evaluation of 3D crack growth using ZENCRACK*. Tech. rep. DTIC Document, 2001.

[43] M. A. Hussain, S. L. Pu, and J. Underwood. “Strain Energy Release Rate for a Crack Under Combined Mode I and Mode II”. In: *Fracture analysis* 560 (1974), pp. 2–28.

[44] V. Infante and J. Silva. “Case studies of computational simulations of fatigue crack propagation using finite elements analysis tools”. In: *Engineering Failure Analysis* 18.2 (2011), pp. 616–624. ISSN: 13506307.

[45] C. E. Inglis. “Stresses in a plate due to the presence of cracks and sharp corners”. In: *Spie Milestone series MS* 137 (1913), pp. 3–17.

[46] L. M. Kachanov. “Time of the rupture process under creep conditions”. In: *Izv Akad Nauk S S R Otd Tech Nauk* 8 (1958), pp. 26–31.

[47] M. Kachanov. “A simple technique of stress analysis in elastic solids with many cracks”. In: *International Journal of Fracture* 28.1 (1985), R11–R19.

[48] M. Kachanov. “Elastic solids with many cracks: A simple method of analysis”. In: *International Journal of Solids and Structures* 23.1 (1987), pp. 23–43. ISSN: 00207683.

[49] M. Kachanov. “On the problems of crack interactions and crack coalescence”. In: *International Journal of Fracture* 120.3 (2003), pp. 537–543. ISSN: 03769429.

[50] Ł. Kaczmarczyk, M. M. Nezhad, and C. Pearce. “Three-dimensional brittle fracture: Configurational-force-driven crack propagation”. In: *International Journal for Numerical Methods in Engineering* 97.7 (2014), pp. 531–550. ISSN: 00295981. arXiv: 1304.6136.

[51] B. L. Karihaloo and L. M. Keer. “Approximate description of crack kinking and curving”. In: *Journal of Applied Mechanics* September 1981 (1981), pp. 515–519.

[52] B. L. Karihaloo, L. M. Keer, and S. Nemat-Nasser. “Crack kinking under non-symmetric loading”. In: *Engineering Fracture Mechanics* 13.4 (1980), pp. 879–888. ISSN: 0013-7944.

[53] T. Lee, M. Leok, and N. H. McClamroch. “Comparison of a phase-field model and of a thick level set model for brittle and quasi-brittle fracture”. In: *Proceedings of the 2011 American Control Conference* February (2011), pp. 1885–1891. ISSN: 0743-1619. arXiv: 1010.1724.

[54] D. Leguillon. “A criterion for crack nucleation at a notch in homogeneous materials”. In: *Comptes Rendus de l’Académie des Sciences - Series IIB - Mechanics* 329.2 (2001), pp. 97–102. ISSN: 16207742.

[55] D. Leguillon. “Strength or toughness? A criterion for crack onset at a notch”. In: *European Journal of Mechanics - A/Solids* 21.1 (2002), pp. 61–72. ISSN: 09977538.

[56] E. Lorentz and S. Andrieux. “A variational formulation for nonlocal damage models”. In: *International Journal of Plasticity* 15.2 (1999), pp. 119–138. ISSN: 07496419.

[57] E. Lorentz and S. Andrieux. “Analysis of non-local models through energetic formulations”. In: *International Journal of Solids and Structures* 40.12 (2003), pp. 2905–2936. ISSN: 00207683.

[58] A. Maligno, C. Soutis, and V. Silberschmidt. “An advanced numerical tool to study fatigue crack propagation in aluminium plates repaired with a composite patch”. In: *Engineering Fracture Mechanics* 99 (2013), pp. 62–78. ISSN: 00137944.

[59] J. J. Marigo. “Initiation of Cracks in Griffith’s Theory: An Argument of Continuity in Favor of Global Minimization”. In: *Journal of Nonlinear Science* 20.6 (2010), pp. 831–868. ISSN: 0938-8974.

[60] G. D. Maso, G. A. Francfort, and R. Toader. “Quasistatic Crack Growth in Nonlinear Elasticity”. In: *Archive for Rational Mechanics and Analysis* 176.2 (2005), pp. 165–225. ISSN: 0003-9527. arXiv: `arXiv:1604.08338v1`.

[61] Y. G. Matvienko. “Maximum average tangential stress criterion for prediction of the crack path”. In: *International Journal of Fracture* 176.1 (2012), pp. 113–118. ISSN: 03769429.

[62] A. Menk and S. P. Bordas. “Crack growth calculations in solder joints based on microstructural phenomena with X-FEM”. In: *Computational Materials Science* 50.3 (2011), pp. 1145–1156. ISSN: 09270256.

[63] A. Menk and S. P. A. Bordas. “A robust preconditioning technique for the extended finite element method”. In: *International Journal for Numerical Methods in Engineering* 85.13 (2011), pp. 1609–1632. ISSN: 00295981. arXiv: `1010.1724`.

[64] A. Menk and S. P. A. Bordas. “Numerically determined enrichment functions for the extended finite element method and applications to bi-material anisotropic fracture and polycrystals”. In: *International Journal for Numerical Methods in Engineering* March (2010), n/a–n/a. ISSN: 00295981.

[65] A. Mesgarnejad, B. Bourdin, and M. M. Khonsari. “Validation simulations for the variational approach to fracture”. In: *Computer Methods in Applied Mechanics and Engineering* 290 (2015), pp. 420–437. ISSN: 00457825.

[66] C. Miehe, F. Welschinger, and M. Hofacker. *Thermodynamically consistent phase-field models of fracture: Variational principles and multi-field FE implementations*. 2010. arXiv: `1010.1724`.

[67] C. Miehe, M. Hofacker, and F. Welschinger. “A phase field model for rate-independent crack propagation: Robust algorithmic implementation based on operator splits”. In: *Computer Methods in Applied Mechanics and Engineering* 199.45-48 (2010), pp. 2765–2778. ISSN: 00457825.

[68] C. Miehe and S. Mauthe. “Phase field modeling of fracture in multi-physics problems. Part III. Crack driving forces in hydro-poro-elasticity and hydraulic fracturing of fluid-saturated porous media”. In: *Computer Methods in Applied Mechanics and Engineering* 304.2015 (2016), pp. 619–655. ISSN: 00457825.

[69] N. Moës, C. Stolz, and N. Chevaugeon. “Coupling local and non-local damage evolutions with the Thick Level Set model”. In: *Advanced Modeling and Simulation in Engineering Sciences* 1.1 (2014), p. 16. ISSN: 2213-7467.

[70] N. Moës et al. “A level set based model for damage growth: The thick level set approach”. In: *International Journal for Numerical Methods in Engineering* 86.3 (2011), pp. 358–380. ISSN: 00295981. arXiv: `1010.1724`.

[71] S. G. Mogilevskaya. “Numerical modeling of 2-D smooth crack growth”. In: *International Journal of Fracture* 87.4 (1997), pp. 389–405. ISSN: 03769429.

[72] S. G. Mogilevskaya. "The universal algorithm based on complex hypersingular integral equation to solve plane elasticity problems". In: *Computational Mechanics* 18.2 (1996), pp. 127–138. ISSN: 0178-7675.

[73] K. Moreau et al. "Explicit dynamics with a non-local damage model using the thick level set approach". In: *International Journal for Numerical Methods in Engineering* 102.3-4 (2015), pp. 808–838. ISSN: 00295981.

[74] A. Munjiza, K. R. F. Andrews, and J. K. White. "Combined single and smeared crack model in combined finite-discrete element analysis". In: *International Journal for Numerical Methods in Engineering* 44.1 (1999), pp. 41–57. ISSN: 0029-5981.

[75] A. Munjiza, D. Owen, and N. Bicanic. "A combined finitediscrete element method in transient dynamics of fracturing solids". In: *Engineering Computations* 12.2 (1995), pp. 145–174. ISSN: 0264-4401.

[76] A. A. Munjiza. *The Combined Finite-Discrete Element Method*. John Wiley & Sons, 2004, p. 352. ISBN: 9780470841990.

[77] S. Murakami. *Continuum Damage Mechanics*. Vol. 185. Solid Mechanics and Its Applications. Dordrecht: Springer Netherlands, 2012. ISBN: 978-94-007-2665-9.

[78] S. Nemat-Nasser and H. Horii. "Compression-induced nonplanar crack extension with application to splitting, exfoliation, and rockburst". In: *Journal of Geophysical Research* 87.B8 (1982), p. 6805. ISSN: 0148-0227.

[79] Q. S. Nguyen and S. Andrieux. "The non-local generalized standard approach: a consistent gradient theory". In: *Comptes Rendus Mécanique* 333.2 (2005), pp. 139–145. ISSN: 16310721.

[80] J. Nocedal and S. J. Wright. *Numerical Optimization*. Ed. by P. Glynn and S. M. Robinson. Vol. 11. 1. Springer, 1999, p. 198. ISBN: ISBN 0-387-98793-2.

[81] V. Novozhilov. "On a necessary and sufficient criterion for brittle strength". In: *Journal of Applied Mathematics and Mechanics* 33.2 (1969), pp. 201–210. ISSN: 00218928.

[82] R Ogden. *Non-linear elastic deformations*. Vol. 1. Dover Civil and Mechanical Engineering 2. Dover Publications, 1984, p. 119. ISBN: 0486696480.

[83] S. Osher, R. Fedkiw, and K. Piechor. *Level set methods and dynamic implicit surfaces*. Vol. 57. 3. 2004, B15. ISBN: 0387954821.

[84] S. Osher and R. P. Fedkiw. "Level Set Methods: An Overview and Some Recent Results". In: *Journal of Computational Physics* 169.2 (2001), pp. 463–502. ISSN: 00219991.

[85] K. Palaniswamy and W. G. Knauss. "Propagation of a crack under general, in-plane tension". In: *International Journal of Fracture Mechanics* 8.1 (1972), pp. 114–117. ISSN: 0020-7268.

[86] A. Parrilla Gómez, N. Moës, and C. Stolz. "Comparison between thick level set (TLS) and cohesive zone models". In: *Advanced Modeling and Simulation in Engineering Sciences* 2.1 (2015), p. 18. ISSN: 2213-7467.

[87] B. Patzak and M. Jirasek. "Process zone resolution by extended finite elements". In: *Engineering Fracture Mechanics* 70 (2003), pp. 957–977. ISSN: 00137944.

[88] R. H. J. Peerlings et al. “Some observations on localisation in non-local and gradient damage models”. In: *European Journal of Mechanics a-Solids* 15.6 (1996), pp. 937–953.

[89] G. Pijaudier-Cabot and N. Burlion. “Damage and localisation in elastic materials with voids”. In: *Mechanics of Cohesive-frictional Materials* 1.2 (1996), pp. 129–144. ISSN: 1082-5010.

[90] R. M. Pradeilles-Duval and C. Stolz. “Mechanical transformations and discontinuities along a moving surface”. In: *Journal of the Mechanics and Physics of Solids* 43.1 (1995), pp. 91–121. ISSN: 00225096.

[91] T. Rabczuk and T. Belytschko. “Cracking particles: a simplified meshfree method for arbitrary evolving cracks”. In: *International Journal for Numerical Methods in Engineering* 61.13 (2004), pp. 2316–2343. ISSN: 0029-5981.

[92] T. Rabczuk, S. Bordas, and G. Zi. “A three-dimensional meshfree method for continuous multiple-crack initiation, propagation and junction in statics and dynamics”. In: *Computational Mechanics* 40.3 (2007), pp. 473–495. ISSN: 0178-7675.

[93] T. Rabczuk, S. Bordas, and G. Zi. “On three-dimensional modelling of crack growth using partition of unity methods”. In: *Computers & Structures* 88.23-24 (2010), pp. 1391–1411. ISSN: 00457949.

[94] T. Rabczuk, J.-H. Song, and T. Belytschko. “Simulations of instability in dynamic fracture by the cracking particles method”. In: *Engineering Fracture Mechanics* 76.6 (2009), pp. 730–741. ISSN: 00137944.

[95] T. Rabczuk et al. “A geometrically non-linear three-dimensional cohesive crack method for reinforced concrete structures”. In: *Engineering Fracture Mechanics* 75.16 (2008), pp. 4740–4758. ISSN: 00137944.

[96] T. Rabczuk et al. “A simple and robust three-dimensional cracking-particle method without enrichment”. In: *Computer Methods in Applied Mechanics and Engineering* 199.37-40 (2010), pp. 2437–2455. ISSN: 00457825.

[97] Y. N. Rabotnov. “Creep rupture”. In: *Applied Mechanics*. Berlin, Heidelberg: Springer Berlin Heidelberg, 1969, pp. 342–349.

[98] Y. N. Rabotnov. “On the equation of state of creep”. In: *ARCHIVE: Proceedings of the Institution of Mechanical Engineers, Conference Proceedings 1964-1970 (vols 178-184), Various titles labelled Volumes A to S* 178.31 (1963), pp. 117–122. ISSN: 0367-8849.

[99] L. Ren et al. “Investigation on the Applicability of Several Fracture Criteria to the Mixed Mode Brittle Fractures”. In: *Advances in Mechanical Engineering* 2013 (2013), pp. 1–11. ISSN: 1687-8132.

[100] J. R. Rice. “A path independent integral and the approximate analysis of strain concentration by notches and cracks”. In: 35 (1968), pp. 379–386.

[101] A. Salvadori. “Crack kinking in brittle materials”. In: *Journal of the Mechanics and Physics of Solids* 58.11 (2010), pp. 1835–1846. ISSN: 00225096.

[102] A. Salvadori. “A plasticity framework for (linear elastic) fracture mechanics”. In: *Journal of the Mechanics and Physics of Solids* 56.5 (2008), pp. 2092–2116. ISSN: 00225096.

[103] A. Seweryn. “A non-local stress and strain energy release rate mixed mode fracture initiation and propagation criteria”. In: *Engineering fracture mechanics* (1998), pp. 737–760.

[104] A. Seweryn. “Brittle fracture criterion for structures with sharp notches”. In: *Engineering Fracture Mechanics* 47.5 (1994), pp. 673–681. ISSN: 00137944.

[105] A. Seweryn and A. Łukaszewicz. “Verification of brittle fracture criteria for elements with V-shaped notches”. In: *Engineering Fracture Mechanics* 69.13 (2002), pp. 1487–1510. ISSN: 00137944.

[106] L. S. Sigl and H.-J. Kleebe. “Microcracking in B4C-TiB2 Composites”. In: *Journal of the American Ceramic Society* 78.9 (1995), pp. 2374–2380. ISSN: 0002-7820.

[107] G. C. Sih. *Mechanics of Fracture Initiation and Propagation*. Dordrecht: Springer Netherlands, 1991. ISBN: 978-94-010-5660-1.

[108] G. C. Sih. “Strain-energy-density factor applied to mixed mode crack problems”. In: *International Journal of fracture* 10.3 (1974), pp. 305–321.

[109] A. Simone, C. A. Duarte, and E. Van der Giessen. “A Generalized Finite Element Method for polycrystals with discontinuous grain boundaries”. In: *International Journal for Numerical Methods in Engineering* 67.8 (2006), pp. 1122–1145. ISSN: 0029-5981.

[110] I. Singer-Loginova and H. M. Singer. “The phase field technique for modeling multiphase materials”. In: *Reports on Progress in Physics* 71.10 (2008), p. 106501. ISSN: 0034-4885.

[111] J. H. Song, H Wang, and T Belytschko. “A comparative study on finite element methods for dynamic fracture”. In: *Computational Mechanics, Springer-Verlag* 42.2 (2008), pp. 239–250. ISSN: 0178-7675.

[112] C. Stolz and N. Moës. “A new model of damage: a moving thick layer approach”. In: *International Journal of Fracture* 174.1 (2012), pp. 49–60. ISSN: 0376-9429.

[113] H. Stumpf and K. C. Le. “Variational principles of nonlinear fracture mechanics”. In: *Acta Mechanica* 83.1-2 (1990), pp. 25–37. ISSN: 0001-5970.

[114] H. Talebi, M. Silani, and T. Rabczuk. “Concurrent multiscale modeling of three dimensional crack and dislocation propagation”. In: *Advances in Engineering Software* 80.C (2015), pp. 82–92. ISSN: 09659978.

[115] H. Talebi et al. “A computational library for multiscale modeling of material failure”. In: *Computational Mechanics* 53.5 (2014), pp. 1047–1071. ISSN: 0178-7675.

[116] H. Talebi et al. “Molecular Dynamics/XFEM Coupling by a Three-dimensional Extended Bridging Domain With Applications to Dynamic Brittle Fracture”. In: *International Journal for Multiscale Computational Engineering* 11.6 (2013), pp. 527–541. ISSN: 1543-1649.

[117] A. Tkatchenko and M. Scheffler. “Accurate Molecular Van Der Waals Interactions from Ground-State Electron Density and Free-Atom Reference Data”. In: *Physical Review Letters* 102.7 (2009), p. 073005. ISSN: 0031-9007.

[118] A. Tkatchenko et al. “Accurate and Efficient Method for Many-Body van der Waals Interactions”. In: *Physical Review Letters* 108.23 (2012), p. 236402. ISSN: 0031-9007.

[119] V. Tvergaard and J. W. Hutchinson. “The relation between crack growth resistance and fracture process parameters in elastic-plastic solids”. In: *Journal of the Mechanics and Physics of Solids* 40.6 (1992), pp. 1377–1397. ISSN: 00225096.

[120] Y. Wang and H. Waisman. “From diffuse damage to sharp cohesive cracks: A coupled XFEM framework for failure analysis of quasi-brittle materials”. In: *Computer Methods in Applied Mechanics and Engineering* 299 (2016), pp. 57–89. ISSN: 00457825.

[121] A. Wells. “Crack opening displacements from elastic-plastic analyses of externally notched tension bars”. In: *Engineering Fracture Mechanics* 1.3 (1969), pp. 399–410. ISSN: 00137944.

[122] H. M. Westergaard. “Bearing pressures and cracks”. In: *Journal of Applied Mechanics* 18 (1939), A49–A53.

[123] M. Williams. “On the Stress Distribution at the Base of a Stationary Crack”. In: *ASME Journal of applied mechanics* 24.109 (1957), p. 114.

[124] C. H. Wu. “Fracture under combined loads by maximum energy release rate criterion”. In: *Journal of Applied Mechanics* 45.553 (1978), pp. 553–558.

[125] C. H. Wu. “Maximum-energy-release-rate criterion applied to a tension-compression specimen with crack”. In: *Journal of Elasticity* 8.3 (1978), pp. 235–257. ISSN: 0374-3535.

[126] C. H. Wu. “Elasticity problems of a slender Z-crack”. In: *Journal of Elasticity* 8.2 (1978), pp. 183–205. ISSN: 0374-3535.

[127] E. Wyart et al. “A substructured FE-shell/XFE-3D method for crack analysis in thin-walled structures”. In: *International Journal for Numerical Methods in Engineering* 72.7 (2007), pp. 757–779. ISSN: 00295981.

[128] E Wyart et al. “Substructuring FEXFE approaches applied to three-dimensional crack propagation”. In: *Journal of Computational and Applied Mathematics* 215.2 (2008), pp. 626–638. ISSN: 03770427.

[129] S. Xiao and T. Belytschko. “A bridging domain method for coupling continua with molecular dynamics”. In: *Computer Methods in Applied Mechanics and Engineering* 193.17-20 (2004), pp. 1645–1669. ISSN: 00457825.

[130] X. P. Xu and A. Needleman. “Numerical simulations of fast crack growth in brittle solids”. In: *Journal of the Mechanics and Physics of Solids* 42.9 (1994), pp. 1397–1434. ISSN: 00225096.

[131] Z. Yosibash, A. Bussiba, and I. Gilad. “Failure criteria for brittle elastic materials”. In: *International Journal of Fracture* 1957 (2004), pp. 307–333. ISSN: 03769429.

[132] X.-K. Zhu. “Improved Incremental J-Integral Equations for Determining Crack Growth Resistance Curves”. In: *Journal of Pressure Vessel Technology* 134.5 (2012), p. 051404. ISSN: 00949930.

[133] X. K. Zhu and J. A. Joyce. “Review of fracture toughness (G, K, J, CTOD, CTOA) testing and standardization”. In: *Engineering Fracture Mechanics* 85 (2012), pp. 1–46. ISSN: 00137944.